Solid Earth Discuss., 6, 937–983, 2014
www.solid-earth-discuss.net/6/937/2014/
doi:10.5194/sed-6-937-2014

Solid Earth
Discussions
Open Access

Did Adria rotate relative to Africa?

D. J. J. van Hinsbergen[1], **M. Mensink**[1], **C. G. Langereis**[1], **M. Maffione**[1], **L. Spalluto**[2], **M. Tropeano**[2], **and L. Sabato**[2]

[1]Department of Earth Sciences, Utrecht University, Budapestlaan 4, 3584 CD Utrecht, the Netherlands
[2]Dipartimento di Scienze della Terra e Geoambientali, Universitá degli Studi "Aldo Moro" di Bari, Via E. Orabona 4, 70125, Bari, Italy

Received: 17 March 2014 – Accepted: 18 March 2014 – Published: 28 March 2014

Correspondence to: D. J. J. van Hinsbergen (d.j.j.vanhinsbergen@uu.nl)

Published by Copernicus Publications on behalf of the European Geosciences Union.

Did Adria rotate relative to Africa?

D. J. J. van Hinsbergen et al.

Abstract

The first and foremost boundary condition for kinematic reconstructions of the Mediterranean region is the relative motion between Africa and Eurasia, constrained through reconstructions of the Atlantic Ocean. The Adria continental block is in a downgoing plate position relative to the strongly curved Central Mediterranean subduction-related orogens, and forms the foreland of the Apennines, Alps, Dinarides, and Albanides-Hellenides. It is connected to the African plate through the Ionian Basin, likely with lower Mesozoic oceanic lithosphere. If the relative motion of Adria vs. Africa is known, its position relative to Eurasia can be constrained through the plate circuit, and hard boundary conditions for the reconstruction of the complex kinematic history of the Mediterranean are obtained. Kinematic reconstructions for the Neogene motion of Adria vs. Africa interpreted from the Alps, and from Ionian Basin and its surroundings, however, lead to scenarios involving vertical axis rotation predictions ranging from ~ 0 to 20° counterclockwise. Here, we provide six new paleomagnetic poles from Adria, derived from the Lower Cretaceous to Upper Miocene carbonatic units of the Apulian peninsula (southern Italy). These, in combination with published poles from the Po Plain (Italy), the Istria peninsula (Croatia), and the Gargano promontory (Italy), document a post-Eocene $9.5 \pm 8.7^{\circ}$ counterclockwise vertical axis rotation of Adria. This result provides no support for models invoking significant Africa–Adria rotation differences between the Early Cretaceous and Eocene. The Alpine and Ionian Basin end-member kinematic models are both permitted within the documented rotation range, yet are mutually exclusive. This apparent enigma can be solved only if one or more of the following conditions (requiring future research) are satisfied: (i) Neogene shortening in the western Alps has been significantly underestimated (by as much as 150 km); (ii) Neogene extension in the Ionian Basin has been significantly underestimated (by as much as 420 km); and/or (iii) a major sinistral strike-slip zone has decoupled North and South Adria in Neogene time. Here we present five alternative reconstructions of Adria

SED

6, 937–983, 2014

at 20 Ma that highlight the enigma: they fit the inferred rotation pattern from this study or previously proposed kinematic reconstructions from the surrounding.

1 Introduction

The complex geodynamic evolution of the central Mediterranean region has been dominated by convergent motion between the African and European plates. Rather than being accommodated along a discrete plate boundary, the complex paleogeography of the region led to convergence being accommodated along segmented subduction zones, and to distributed overriding plate shortening. In addition, subduction roll-back since the late Eocene has formed a series of extensional back-arc basins and strongly curved subduction zones and associated mountain belts (e.g., Dewey et al., 1989; Doglioni et al., 1997; Gueguen et al., 1998; Jolivet et al., 2009; Rosenbaum and Lister, 2004; Stampfli and Hochard, 2009; Wortel and Spakman, 2000). It is this complex evolution that has made the Mediterranean region instrumental in the development of fundamental concepts that link surface deformation to deep mantle processes (Carminati et al., 2012; Cavazza et al., 2004; Doglioni, 1991; Faccenna and Becker, 2010; Govers and Wortel, 2005; Jolivet et al., 2009; Malinverno and Ryan, 1986; Wortel and Spakman, 2000).

Detailed kinematic reconstructions constitute a fundamental tool for advancing our understanding of the complex geodynamics of the Mediterranean region. A common boundary condition adopted by all reconstructions is represented by the relative motions summarized in the Eurasia–North America–Africa plate circuit based on marine magnetic anomalies of the Atlantic Ocean (e.g., Capitanio and Goes, 2006; Dewey and Sengör, 1979; Dewey et al., 1989; Gaina et al., 2013; Rosenbaum et al., 2002; Savostin et al., 1986; Seton et al., 2012; Torsvik et al., 2012; Vissers et al., 2013), which defined the area generated and consumed between Africa and Europe since the break-up of Pangea. A critical element in Mediterranean reconstructions is the continental domain of Adria (Fig. 1). Adria is a fragment of continental crust intervening the

SED
6, 937–983, 2014

European and African plates composed of essentially undeformed platform carbonates currently exposed on the Apulia peninsula and Gargano promontory of southern Italy, the Istria peninsula of Croatia, and the Adige Embayment of the southern Alps. Adria is in a downgoing plate position relative to all surrounding mountain belts: it is overthrust by the Apennines in the west and the Dinarides-Albanides-Hellenides in the east, and although it was originally in an overriding plate position in the Alps, it became overthrust by these since Neogene time. Tectonic slices of the Adriatic upper crust are currently exposed in all circum-Adriatic mountain ranges (Bernoulli and Jenkyns, 2009; Faccenna et al., 2001; Gaina et al., 2013; Handy et al., 2010; Schmid et al., 2008; Stampfli and Hochard, 2009; Stampfli and Mosar, 1999; Ustaszewski et al., 2008; Vai and Martini, 2001; van Hinsbergen and Schmid, 2012) (Fig. 1). To the south, Adria is separated from the North African passive continental margin by oceanic lithosphere of the Ionian Basin (Catalano et al., 2001; Frizon de Lamotte et al., 2011; Gallais et al., 2011; Speranza et al., 2012).

There is no zone of intense compression between Adria and Africa, and Adria has been paleolatitudinally stable relative to Africa within paleomagnetic error bars (of typically several hundreds of kilometres) (e.g., Channell et al., 1979; Rosenbaum et al., 2004). Because the motion of Adria relative to Europe would be the best boundary condition to reconstruct the central Mediterranean kinematic history since the Mesozoic, it is crucial to reconstruct any past relative motions between Adria and Africa. Different approaches to this end, however, lead to contrasting results. The Ionian Basin's sea floor is widely regarded as Mesozoic (e.g., Catalano et al., 2001; Frizon de Lamotte et al., 2011; Gallais et al., 2011; Schettino and Turco, 2011; Speranza et al., 2012), implying a semi-rigid connection between Adria and Africa since that time. Eastward increasing Neogene shortening in the Alps (Schmid et al., 2013; Schönborn, 1999), however, has been used to infer a Neogene $\sim 20^{\circ}$ counterclockwise (ccw) rotation of Adria relative to Eurasia (Ustaszewski et al., 2008), only $\sim 2^{\circ}$ of which can be accounted for by African–Europe plate motion. That would suggest that Adria was decoupled from Africa during the Neogene. GPS measurements suggest that at present, Adria moves

NE-ward motion relative to Africa (D'Agostino et al., 2008). These present-day kinematics are consistent with a NE-ward motion of Adria vs. Africa of 40 km over the past 4 Myr inferred from kinematic reconstruction of the Aegean region (van Hinsbergen and Schmid, 2012). Conversely, Wortmann et al. (2007) argued for a Cenozoic 8° clockwise (cw) rotation of Adria vs. Africa to avoid overlaps of Adria with Eurasia in pre-Cenozoic reconstructions, and Dercourt et al. (1986) postulated a 30° ccw rotation of Adria relative to Africa between 130 and 80 Ma, assuming a Cretaceous opening of the Ionian Basin.

Paleomagnetic data can provide useful quantitative constraints on the vertical axis rotation history of Adria. Contrasting results from the above-mentioned regions exposing Adria's sedimentary cover, however, have been reported, interpreted to reflect (i) no rotation (Channell, 1977; Channell and Tarling, 1975), (ii) 20° cw rotation since 30 Ma (Tozzi et al., 1988), (iii) 20° ccw rotation since the late Cretaceous (Márton and Nardi, 1994), or (iv) more complex models where a 20° ccw early-late Cretaceous rotation was followed by a late Cretaceous–Eocene 20° cw rotation and a post-Eocene 30° ccw rotation (Márton et al., 2010).

In this paper, we present a new paleomagnetic study of the Lower Cretaceous to Upper Miocene stratigraphy of the Apulian carbonate platform (southern Italy). We compare our results to, and integrate these with published data sets and evaluate the range of paleomagnetically permissible rotations values in terms of their kinematic consequences for Central Mediterranean region reconstructions.

2 Geological setting

Before the onset of Africa–Europe convergence in the mid-Mesozoic, Adria was much larger than today and stretched from the Italian Alps to Turkey (Vlahoviæ et al., 2005). Gaina et al. (2013) introduced the term "Greater Adria" for all continental lithosphere including many Mesozoic intracontinental rift basins and platforms that are now incor-

SED
6, 937–983, 2014

porated in the surrounding fold-thrust belts and that existed between the Vardar ocean (or Neotethys) and the Ionian Basin.

Greater Adria was separated from Eurasia in the northeast by the Triassic Vardar, or Neo-Tethys Ocean (Gaina et al., 2013; Schmid et al., 2008) and in the north and west by the Jurassic Piemonte Ligurian, or Alpine Tethys Ocean (e.g., Favre and Stampfli, 1992; Frisch, 1979; Handy et al., 2010; Rosenbaum and Lister, 2005; Vissers et al., 2013). To the south the Ionian Basin separated Adria from Africa (Fig. 1). Adria's conjugate margin across the Ionian Basin is likely the Hyblean Plateau of Sicily bounded to the east by the Malta escarpment (Catalano et al., 2001; Chamot-Rooke and Rangin, 2005; Speranza et al., 2012).

Before the Calabrian subduction zone retreated away from Sardinia in the late Miocene (Cifelli et al., 2007; Faccenna et al., 2001, 2004; Rosenbaum et al., 2008), the Ionian Basin extended farther to the north-west. This oceanic lithosphere was at least Jurassic in age, as evidenced by off-scraped sediments now exposed in Calabria (Bonardi et al., 1988). The modern Ionian Basin is floored by a > 5 km thick sequence of sediments, which in the west have been thrust in response to subduction below Calabria (the Calabrian accretionary prism), and in the east in response to subduction below the Aegean region (the "Mediterranean ridge") (e.g., Finetti, 1985; Gallais et al., 2011; Minelli and Faccenna, 2010; Reston et al., 2002; Speranza et al., 2012). The Ionian abyssal plain is the only relatively undeformed portion that serves as the foreland of the central Mediterranean subduction systems (Gallais et al., 2011; Hieke et al., 2006; Speranza et al., 2012). Given the crustal thickness of 7–9 km (Chamot-Rooke and Rangin, 2005) and very low heatflow (Pasquale et al., 2005) this ocean floor is likely oceanic in nature, and very old (e.g., Gallais et al., 2011; Speranza et al., 2012). The age of the Ionian Basin has been estimated to range from late Paleozoic to Cretaceous (Dercourt et al., 1986; Frizon de Lamotte et al., 2011; Gallais et al., 2011; Golonka, 2004; Robertson et al., 1991; Schettino and Turco, 2011; Sengör et al., 1984; Stampfli and Borel, 2002), with the most recent suggestion giving a late Triassic age (Speranza et al., 2012).

SED
6, 937–983, 2014

Despite the uncertainties on the opening age and direction (NE–SW according to Chamot-Rooke and Rangin (2005) and Speranza et al. (2012) or NW–SE according to Frizon de Lamotte et al. (2011) and Gallais et al. (2011), there is general agreement that the Ionian abyssal plane has not been strongly deformed since the middle Mesozoic. Minor late Miocene inversion was associated with only a few kilometers of shortening (Gallais et al., 2011). Also the Malta escarpment has not been reactivated after the Mesozoic, and gently dips towards the basin floor, except to the northwest where the margin is reactivated in Pliocene and younger times, likely as a STEP fault accommodating Calabrian trench retreat (Argnani and Bonazzi, 2005). Late Miocene and younger NE–SW extension, however, has been documented within the African passive margin, forming the ~140 km wide Sicily Channel rift zone (Argnani, 2009) between Sicily and the Tunisian coast (Fig. 1). This rift system is associated with up to ~40 % crustal thinning and contains active rift-related volcanoes (Civile et al., 2008). The dimension of the rifted zone and the crustal attenuation may indicate some tens of kilometers of extension. This system connects to the SE to the Sirte and Tripolitana basins of Lybia (Capitanio et al., 2011) and was interpreted to reflect renewed late Miocene and younger NE–SW extension between Adria (and the Ionian Basin), and Africa, likely caused by slab-pull forces of the subducting African plate (Argnani, 1990; Belguith et al., 2013; Capitanio et al., 2011; Civile et al., 2010; Goes et al., 2004).

Our study area, the Apulian carbonate platform, herafter called “Apulia” (Fig. 2), is part of Adria and lies in the Plio-Pleistocene foreland of the Apennine fold-thrust belt to the west (D’Argenio et al., 1973). Recent NE–SW, low-magnitude extension evident from Apulia (Fig. 2) is interpreted to result from flexural bending of the down-going Adriatic lithosphere into the Apennine subduction zone (Argnani et al., 2001; Doglioni et al., 1994). To the northeast, Apulia borders the Adriatic Sea, which represents the Late-Miocene-Quaternary foredeep of the Dinarides-Albanides-Hellenides belt (Argnani, 2013; Argnani et al., 1996; Bertotti et al., 2001; de Alteriis, 1995). The southwestern margin of Apulia appears to constitute a passive margin of the Ionian Basin in a narrow segment between the Calabrian prism and the Mediterranean ridge

SED
6, 937–983, 2014

along the Apulian Escarpment (Finetti, 1985), where accumulation of sediment since the Mesozoic has compensated the thermal subsidence of the oceanic lithosphere (Channell et al., 1979; Ricchetti et al., 1998).

The northern margin of the platform is exposed on the Gargano promontory that was located close to the northestern transition of Apulia toward the adjacent Adriatic Basin (Bosellini et al., 1999b; Graziano et al., 2013; Santantonio et al., 2013). The Adriatic Basin, from which the present-day Adriatic Sea roughly inherited the location, was a Jurassic deep water continental rift basin that continued northwestward into the Umbria-Marche basin, now incorporated in the Apennine fold-thrust belt, and southeastward into the Ionian Zone which is now part of the Hellenides-Albanides and should not be confused with the previously mentioned oceanic Ionian Basin, located on the opposite side of Apulia (Fantoni and Franciosi, 2010; Flores et al., 1991; Grandic et al., 2002; Mattavelli et al., 1991; Picha, 2002; Zappaterra, 1990, 1994). Basin-transition units of Apulia have in Pliocene and younger times become incorporated in the Pre-Apulian zone of western Greece, exposed on the Ionian Islands which became separated from Apulia along the Kefallonia Fault Zone (Kokkalas et al., 2013; Royden and Papanikolaou, 2011; Underhill, 1989; van Hinsbergen et al., 2006).

To the north of Apulia, in the central Adriatic Sea, the fronts of the external Dinarides and Apennines antithetically meet, producing the Mid-Adriatic Ridge (Fig. 1). There, the Adriatic Basin is cut by Neogene NW–SE striking thrusts, some of which invert Mesozoic extensional structures (Fantoni and Franciosi, 2010; Grandic et al., 2002; Kastelic et al., 2013; Scisciani and Calamita, 2009; Scrocca, 2006). South of the Mid-Adriatic Ridge, it is believed that several strike-slip structures, about W–E or SW–NE striking, dissect the Adriatic Basin; unlikely, Authors disagree with each other about the location or the movement of these structures (although primarily considered dextral in origin), whose presence is mainly inferred from the analysis of seismicity, low-resolution seismic lines, or GPS velocities. As a result, three main deformation zones, alternative to each other, were called into consideration to decouple North and South Adria: (i) the first one is the Pescara–Dubrovnik line, whose presence was hypotesized by Gambini and Tozzi (1996), and that roughly corresponds to a segment of the boundary that, according to Oldow et al. (2002), borders two fragments of Adria with different GPS-measured velocity; (ii) the second one is the Tremiti Line of Finetti (1982) or the Tremiti Structure of Andre and Doulcet (1991), whose presence is well known for both its seismicity (Favali et al., 1993, 1990) and sea-floor deformation (Argnani et al., 1993). According to Doglioni et al. (1994) and Scrocca (2006), this dextral lithospheric structure segments Adria in order to accommodate a differential slab retreat, and, according to Festa et al. (2014), its subsurface evidences were enhanced by salt tectonics; (iii) finally, also the Mid-Adriatic Ridge was interpreted to be a boundary between two different sectors of Adria (Scisciani and Calamita, 2009), assuming that some structural highs of the external Dinarides (i.e. the Palagruza High of Grandic et al., 2002) represent the southward prosecution of the same ridge in the estern Adriatic Sea.

Apulia was considered an isolated carbonate platform that developed away from emerged continents (D'Argenio et al., 1973) until the discovery of dinosaur footprints that suggested the presence of some continental bridges between Apulia and other coeval exposed regions in Late Jurassic to Early Cretaceous time (e.g. Bosellini, 2002). During the Mesozoic, shallow water carbonate deposition was able to compensate the regional subsidence, and led to the accumulation of a stratigraphic succession up to 6000 m thick (Ricchetti et al., 1998). The succession, whose Cretaceous interval is widely exposed, consists mainly of dolomitic and calcareous rocks (Ricchetti, 1975). In the Murge area (Fig. 2), where its age has been best constrained (Spalluto, 2011; Spalluto and Caffau, 2010; Spalluto et al., 2005), the succession forms a monocline dipping gently towards the SSW, thus exposing younger rocks from NNE to SSW (Ciaranfi et al., 1988) (Fig. 2). This monoclinal succession is deformed by gentle undulations and steep normal and transtensional faults with an overall NW–SE orientation (Festa, 2003). The southernmost part of the exposed Apulia (i.e. the edge of the Salento Peninsula facing the Otranto Channel, Fig. 2) represents the position of the Mesozoic platform margin (Bosellini et al., 1999b). It probably sharply passed to a southern intraplatform pelagic basin, recognized in the subsurface of the submerged

Apulia (Del Ben et al., 2010). Post Cretaceous carbonate rocks cropping out along this Salento margin show well-preserved tens of meters thick clinoforms, i.e slope deposits that formed along and rework rocks of the old Apulia margin (Bosellini et al., 1999b). These slope deposits reach up to 25/30° of primary non-tectonic dip (Bosellini, 2006; Tropeano et al., 2004).

3 Paleomagnetic sampling, analysis and results

3.1 Sampling and laboratory treatment

We collected 456 samples from nine localities covering the Cretaceous and Cenozoic carbonate stratigraphy of Apulia. Cores samples were collected with a gasoline powered motor drill and their orientation was measured with a magnetic compass.

The samples were measured at the Paleomagnetic Laboratory Fort Hoofddijk of Utrecht University, the Netherlands. The nature of the magnetic carriers was investigated for representative samples using an in-house developed horizontal translation type Curie balance, with a sensitivity of 5×10^{-9} A m^2 (Mullender et al., 1993). Approximately 60 mg of powder obtained from each sample was subjected to stepwise heating-cooling cycles up to 700 °C.

For each locality, eight to ten samples were selected as pilot samples, and of each sample two specimens were retrieved for both thermal (TH) and alternating field (AF) demagnetization. AF demagnetization and measurement of the remanence were carried out using an in-house developed robotized sample handler coupled to a horizontal pass-through 2G Enterprises DC SQUID cryogenic magnetometer (noise level 1×10^{-12} A m^2) located in a magnetically shielded room (residual field < 200 nT). Samples were demagnetized by stepwise AF treatment (alternating field steps: 5, 8, 12, 15, 20, 25, 30, 35, 40, 45, 50, 60, 70, 80 and 100 mT). Thermal demagnetizations were performed in a magnetically shielded oven using variable temperature increments up to 500 °C. After each heating step the remanence was measured with a 2G Enterprises horizontal 2G DC SQUID cryogenic magnetometer (noise level 3×10^{-12} A m^2).

Thermal demagnetization treatment demonstrated to be more effective for the sampled rocks as it provided more stable demagnetization diagrams than the AF technique. The remaining samples of each locality were therefore thermally demagnetized.

Demagnetization diagrams were plotted on orthogonal vector diagrams (Zijderveld, 1967) and the characteristic remanent magnetizations (ChRMs) were isolated via principal component analysis (Kirschvink, 1980). Samples with a maximum angular deviation (MAD) larger than 15° were rejected from further analysis. Because secular variation of the geomagnetic field induces scatter in paleomagnetic directions whose distribution gradually becomes more ellipsoidal towards equatorial latitudes (Creer et al., 1959; Tauxe and Kent, 2004), we calculated site mean directions using (Fisher, 1953) statistics on virtual geomagnetic poles (VGPs) following procedures described in (Deenen et al., 2011). At each locality a 45° cut-off was applied to the VGPs (Johnson et al., 2008). The results were then filtered by the paleomagnetic quality criteria of the N-dependent reliability envelope of (Deenen et al., 2011). Mean values and statistical parameters are listed in Table 1.

3.2 Results

Curie balance results are noisy because of the very low intensities of these carbonates, and do no not reveal meaningful information about the carriers of the remanence. Upon close inspection it can be seen that some new magnetic mineral is created upon heating, just above 400 °C. This points to the presence of minor amounts of pyrite converted to magnetite. The cooling curves are higher than the heating curves, confirming that new magnetic minerals were created that were not fully removed upon heating to 700 °C (Fig. 3).

The very low NRM intensities of these limestones also causes nearly 30 % of the demagnetized specimens (167) to show an erratic demagnetization pattern and many samples yielded no interpretable directions. Nevertheless, a total of 298 demagnetized specimens show a weak but stable and measurable remanence. In general, the lowest temperature steps (or AF steps) show a viscous or present-day overprint (Fig. 4). After removing this overprint, the characteristic remanent magnetization (ChRM) directions were interpreted. Most specimens show interpretable results up to temperatures of approximately 400–450 °C. Above this temperature intensities become too low or spurious magnetizations occur that hamper any further interpretation (e.g. Fig. 4g). Of the more succesful demagnetization diagrams, we use eight to ten successive temperature steps for the ChRM directions determined by principal component analysis.

3.2.1 Locality Petraro quarry (PA)

The Petraro quarry (PA) is located in NE Murge close to the town of Barletta (Fig. 2). This section shows the oldest part of the Calcare di Bari Formation cropping out in the Murge area and consists of a well-bedded, 55 m-thick, shallow-water carbonate succession in which few dm-thick carbonate beds are irregularly alternated with a few m-thick dolomitic beds (Luperto-Sinni and Masse, 1984). Carbonate lithofacies are made up of biopeloidal wackestones/packstones and microbial bindstones with rare intercalations of biopeloidal and oolitic grainstones interpreted as formed in inner shelf peritidal environments. Dolomites consists of an anhedral or subhedral mosaic of dolomitic crystals, which totally or partly replaced the carbonate precursor. Based on the study of the microfossiliferous assemblage of PA (mostly benthic foraminifers and calcareous algae), Luperto-Sinni and Masse (1984) refer this succession to the Valanginian (∼ 140–136 Ma; according to the geological time scale of Gradstein et al., 2012). We sampled a 10 m-thick interval of this section avoiding to drill dolomitic beds. The NRM intensity of these samples is very low (30–300 $\mu A\,m^{-1}$) and stable ChRMs were isolated for only 39 specimens at temperature steps between 220 and 500 °C (Fig. 4a–c). The ChRMs show both normal and reverse polarities, and yield a positive reversal test (Johnson et al., 2008; McFadden and McElhinny, 1990) (classification C; $\gamma = 15.9 < \gamma_c = 19.5$). The distribution of the ChRMs satisfies the quality criteria of representing PSV (i.e. $A95_{min} < A95 < A95_{max}$; Deenen et al., 2011). The tilt corrected mean ChRM direction

SED
6, 937–983, 2014

for this locality after a fixed 45° cut-off is $D \pm \Delta D = 130.8 \pm 8.5°$, $I \pm \Delta I = -23.4 \pm 14.6°$ ($N = 29$, $K = 11.5$, $A95 = 10.9°$) (Table 1 and Fig. 5).

3.2.2 Locality Casa Rossa quarry (CR)

The Casa Rossa quarry (CR) is a large limestone quarry in the NE Murge area (Fig. 2), located SW of Trani. The outcropping section consists of a well-bedded, more than 40 m-thick, shallow-water carbonate succession. Similarly to the Petraro quarry, carbonate beds consist of biopeloidal wackestones/packstones and microbial bindstones showing evidence of desiccation features (mud cracks and birdeyes) interpreted as formed in inner shelf peritidal environments. Interbedded with the carbonate lithofacies there are few-mm thick green shale intercalations interpreted as palaeosols. Based on the study of the microfossiliferous assemblage of CR, Luperto-Sinni and Masse (1984) refer this succession to the Barremian to lower Aptian (∼ 129–121 Ma). We sampled a stratigraphic thickness of 20 m in the lower part of the outcropping succession. The low intensity of these rocks (5–100 $\mu A m^{-1}$) did not allow to obtain high quality remanence components because of high MAD values and the distribution of the isolated ChRMs is highly scattered, failing all the adopted quality criteria (Fig. 5). The locality is therefore not considered for further analyses.

3.2.3 Locality Cavallerizza quarry (CU)

The Cavallerizza quarry (CU) is located in the western Murge area (Fig. 2), close to the town of Ruvo di Puglia. The outcropping section shows rudist biogenic beds, late Cenomanian in age (∼ 98–94 Ma), belonging to the uppermost part of the Calcare di Bari Fm (Iannone and Laviano, 1980). Rudist beds are topped by a horizon of green clays, 1 m thick, interpreted as a palaeosol, which marks a regional unconformity covering the whole Turonian (∼ 94–90 Ma). Peritidal limestones of the Calcare di Altamura Fm, Coniacian-Santonian in age (∼ 90–83.5 Ma), overlie green shales and mark the recovery of carbonate marine sedimentation after the Turonian subaerial exposure. A total of 43 samples were collected from the lower, 15 m thick, grey-brown rudist limestones of the Calcare di Bari Fm. According to Laviano et al. (1998), upper Cenomanian rudist beds cropping out in the Ruvo area record the progradation of a rudist-inhabited margin into a shallow intraplatform basin. Samples are characterized by generally low intensities (10–290 $\mu A\,m^{-1}$), but show interpretable demagnetization diagrams (Fig. 4d and e). The mean tilt corrected direction after applying a 45° cut-off to the ChRMs distribution is $D \pm \Delta D = 333.2 \pm 7.1°$, $I \pm \Delta I = 44.9 \pm 8.0°$ ($N = 32$, $K = 16.8$, $A95 = 10.2°$) (Table 1 and Fig. 5). The VGP scatter for this site is consistent with that expected from PSV ($A95_{min} < A95 < A95_{max}$).

3.2.4 Locality Caranna quarry (CN)

The Caranna quarry (CN) is located in SE Murge (Fig. 2), close to the town of Cisternino. The outcropping section consists of an about 20 m-thick succession of thin-bedded pelagic chalky limestones (microbioclastic mudstones to wackestones) containing planktonic foraminifers and calcispheres. According to Pieri and Laviano (1989) and Luperto-Sinni and Borgomano (1989), these deposits formed in relatively deep-water, distal slope environments in late Campanian to early Maastrichtian times (~ 78–69 Ma). All 45 samples were collected from the lower part of the outcropping succession. Only 30 % of the analyzed specimens yielded interpretable demagnetization diagrams because of the low intensity of the NRM (8–34 $\mu A\,m^{-1}$). Stable ChRMs were isolated at low temperatures commonly not exceeding 280 °C (Fig. 4f and g) and their distribution provided a mean value of $D \pm \Delta D = 2.3 \pm 11.8°$, $I \pm \Delta I = 51.7 \pm 10.7°$ ($N = 15$, $K = 15.7$, $A95 = 9.9°$) (Table 1 and Fig. 5). Although the distribution of the ChRMs reflect a PSV-induced scatter, the obtained mean direction is not statistically different from the present day field direction (PDF; Fig. 5) and not consistent with the expected Cretaceous inclinations. It is very likely that a recent magnetic overprint affected this site, and the obtained results are not considered further.

SED
6, 937–983, 2014

3.2.5 Locality Porto Selvaggio cove (PS)

The succession of the Porto Selvaggio cove (PS) crops out in western Salento. It mostly consists of upper Campanian chalky limestones (∼ 78–72 Ma), slightly dipping to the SE, overlying sub-horizontal shallow marine limestones and dolostones (Reina and Luperto-Sinni, 1994a). According to Mastrogiacomo et al. (2012) chalky limestones sampled in this study formed in an intraplatform basin and record the evidence of a syn-sedimentary tectonic activity, as shown by the occurrence of two horizons of soft-sediment deformation structures (slumps). Out of the 52 demagnetized specimens, 48 yielded interpretable diagrams for the calculation of the ChRMs (Fig. 4h and i). The NRM of those samples is characterized by relatively low intensities (10–2000 $\mu A\,m^{-1}$) and and both normal and reversed ChRM's that did not pass the reversal test ($\gamma = 29 > \gamma_c = 14.7$) (McFadden and McElhinny, 1990). The mean normal polarity ChRM shows, after a fixed 45° cut-off, a $D \pm \Delta D = 357.7 \pm 10.3°$, $I \pm \Delta I = 45.4 \pm 11.4°$ ($N = 23$, $K = 10.1$, A95 = 9.2°) (Table 1, Fig. 5), very close to the present-day field, and likely the result of a recent overprint. The reverse polarity ChRMs yield a mean value that is statistically different from the present-day field direction ($D \pm \Delta D = 165.0 \pm 8.9°$, $I \pm \Delta I = -18.4 \pm 16.2°$, $N = 14$, $K = 21.6$, A95 = 8.8°; see Table 1). The distribution of the reverse polarity ChRMs satisfy our criteria. Accordingly, only the reversed polarity ChRM are used for further analyses.

3.2.6 Locality Massafra (MA)

This locality was sampled from a road cut close to the town of Massafra in the south of Murge (Fig. 2). We sampled a 15 m-thick stratigraphic interval mostly comprising well-bedded white to light-brown shallow-water limestones with a Maastrichtian age (72–66 Ma) (Reina and Luperto-Sinni, 1994b). Sampled limestones mostly consist of peritidal, mud-supported, biopeloidal mudstones and wackestones showing a benthic microfossiliferous assemblage (mostly benthic foraminifers and ostracodes). The NRM intensity in those samples is relatively low (0.08–6 $mA\,m^{-1}$) and only 18 samples yielded interpretable demagnetization diagrams (Fig. 4). The mean direction of the isolated ChRMs in tilt-corrected coordinates is $D \pm \Delta D = 8.8 \pm 10.7^{\circ}$, $I \pm \Delta I = 46.6 \pm 11.4^{\circ}$ ($N = 17$, $K = 15.2$, $A95 = 9.4^{\circ}$) (Table 1 and Fig. 5). Before tilt correction, this direction is not statistically different from the present-day field ($D \pm \Delta D = 359.8 \pm 12.6^{\circ}$, $I \pm \Delta I = 52.2 \pm 11.2^{\circ}$, $N = 17$, $K = 12.4$, $A95 = 10.5^{\circ}$) and is probably the effect of a recent overprint. Accordingly, this site is not considered for further analyses.

3.2.7 Locality Torre Specchialaguardia (TS)

An about 10 m-thick succession of clinostratified breccias and bioclastic deposits was sampled at the Torre Specchialaguarda locality (TS) in E Salento (Fig. 2). This succession belongs to the Upper Eocene (Priabonian, 44–38 Ma) Torre Specchialaguardia Limestone Fm (Parente, 1994), which formed in a steep forereef slope onlapping a rocky Cretaceous to Eocene paleocliff (Bosellini et al., 1999b). According to Parente (1994) and Bosellini et al. (1999b), this formation is the oldest non-deformed unit in eastern Salento and its current dip of $\sim 30^{\circ}$ to the ESE is a primary, non-tectonic orientation. A total of 56 samples yielded NRM intensities ranging between 0.15 and 3 $\mathrm{mA\,m^{-1}}$ and usually gave stable demagnetization diagrams characterized by curie temperatures around 420 °C (Fig. 4l–n). The remanence displays both normal and reverse polarities that pass the reversal test (McFadden and McElhinny, 1990) (classification C, $\gamma = 8.2 < \gamma_c = 11.7$). After a fixed 45° cut-off, the mean in situ ChRM direction is $D \pm \Delta D = 356.0 \pm 5.6^{\circ}$, $I \pm \Delta I = 44.8 \pm 6.3^{\circ}$ ($N = 47$, $K = 17.9$, $A95 = 5.1^{\circ}$) (Table 1, Fig. 5) and the ChRMs distribution satisfies our criteria.

3.2.8 Locality Castro (OC)

An about 10 m-thick section was sampled close to the village of Castro (OC) in E Salento (Fig. 2). The outcropping succession consists of Upper Oligocene (Chattian, 28–23 Ma) limestones belonging to the Castro Limestone Fm (Bosellini and Russo, 1992; Parente, 1994). This unit represents a fringing reef complex and shows a very well-preserved lateral zonation of the reef subenvironments (Bosellini and Russo, 1992; Parente, 1994). The sampled section shows clinostratified bioclastic deposits belonging to the reef slope subenvironment showing no evidence of tectonic deformation (Bosellini and Russo, 1992). Very low NRM intensities characterize these rocks (15–180 μA m^{-1}) and stable ChRM components with maximum unblocking temperatures between 220–500 °C were isolated from 31 specimens (Fig. 4o and p). The mean ChRM direction after a fixed 45° cut-off is $D \pm \Delta D = 180.5 \pm 3.2°$, $I \pm \Delta I = -44.2 \pm 3.7°$ ($N = 29$, $K = 85.8$, $A95 = 2.9°$) (Table 1 and Fig. 5). The VGP distribution does not entirely satisfy our criteria, since the A95 value is lower than $A95_{min}$, indicating that PSV is underrepresented. The reverse polarity of the ChRMs and their low inclinations excludes a present-day (or recent) overprint, and the underrepresentation of PSV may be the result of some averaging PSV within each limestone sample.

3.2.9 Locality Novaglie (MN1–3)

Three different sites belonging to the Lower Messinian succession of the Novaglie Fm were sampled within three km of each other, close to the eastern Salento coast (Fig. 2). The outcropping successions consist of in situ coral reef bioconstructions, clinostratified breccias and associated bioclastic and lithoclastic prograding slope deposits and fine-grained, bioclastic base-of-slope calcarenites. Similarly to the previous two localities, the bedding attitude in the sampled sites is most likely primary (Bosellini et al., 1999a, b, 2001; Vescogni, 2000). At each sub-site 20 samples were collected from a 10 m-thick interval. NRM intensities range between 9 and 5000 μA m^{-1}. A total of 16, 13, and 6 ChRMs were successfully isolated from sub-site MN1, MN2, and MN3, respectively (Fig. 4q–s). Overall, the direction of the isolated ChRMs is substantially scattered, with both normal and reverse polarities. The reversal test yielded a negative result (McFadden and McElhinny, 1990), therefore separate mean values were calculated at each sub-site.

After a fixed 45° cut-off, site MN1 yielded a mean paleomagnetic direction of $D \pm \Delta D = 355.1 \pm 12.5°$, $I \pm \Delta I = 61.1 \pm 7.9°$ ($N = 14$, $K = 19.5$, $A95 = 9.2°$) (Table 1, Fig. 5). The

VGP distribution passes our quality criteria. Only 6 specimens of MN 2 yielded a poorly-defined ChRM, with a dispersion well beyond our quality criteria (Fig. 5). This sub-site was discarded. The large scatter of the ChRMs of sub-site MN3 yields, after the 45° cut-off, eight samples with a mean ChRM of $D \pm \Delta D = 222.5 \pm 13.7°$, $I \pm \Delta I = -33.2 \pm 20.2°$ ($N = 8$, $K = 19.0$, A95 = 13.0°) (Table 1, Fig. 5). Despite the low number of specimens, the A95 envelope passes the (Deenen et al., 2011) criteria (Table 1).

4 Discussion

4.1 Paleomagnetic constraints on the rotation of Adria

Reliable paleomagnetic poles were obtained from six localities (out of nine) sampled throughout Apulia (Fig. 2). The results from three localities were discarded because the distribution of the isolated ChRMs did not match the adopted quality criteria or because of a present-day overprint. One more site (MN3), although passing the quality criteria, yielded an anomalous declination (042.5 ± 13.7°) indicating a strong clockwise rotation, not seen in the rest of the reliable sites. The anomalous direction at site MN3 may be explained considering that the samples, collected in a forereef breccia, could represent a large fallen block within the Messinian slope deposits. Regardless of the cause of this local rotation, we consider this direction not meaningful for the analysis of the regional rotation of Adria.

The rotation of Adria and its relationship with the African plate has always been a moot point (Márton et al., 2003, 2008; Caporali et al., 2000). Our new data provide new constraints for the rotation of Adria during the Cenozoic and, more importantly, can test the robustness and reliability of the available dataset. Interestingly, we can compare the results of the Oligocene site OC (Fig. 2) with those obtained by Tozzi et al. (1988) from the same area. These authors interpreted the local ~ 30° ESE-ward bedding dip as a result of tectonic tilting, inconsistent with sedimentological studies (e.g., Bosellini, 2006), and calculated a post-Paleogene ~ 25° cw rotation of Adria by restoring this bedding to the horizontal. The paleomagnetic direction should be interpreted in in situ coordinates, and our results as well as those of Tozzi et al. (1988) are coincident and indicate no, or a minor counterclockwise post-Oligocene rotation of Adria with respect to Africa (Fig. 6).

To assess whether and when Adria rotated relative to Africa, we combine our results with published data from Apulia, Gargano, Istria and the Adige Embayment, and compare them to the expected directions for the European and African plates calculated from the Global APWP of Torsvik et al. (2012) using a reference location of 40.7° N, 17.2° E (Table 1, Fig. 7). Mean paleomagnetic directions and statistical parameters from the existing database were re-calculated at each site by averaging VGPs obtained through parametric bootstrap sampling using the provided mean values and statistical parameters (Table 1). This procedure overcomes the loss of information on the original data scatter that occurs when only the mean paleomagnetic direction at a given locality is computed by averaging site averages. In addition, sites with different numbers of samples should weigh differently, since large datasets provide a better representation of PSV than small data sets (see Deenen et al., 2011).

The updated paleomagnetic database is composed of twelve poles from Apulia (Márton and Nardi, 1994; Scheepers, 1992; Tozzi et al., 1988), five from the Gargano promontory (Channell, 1977; Channell and Tarling, 1975; Speranza and Kissel, 1993; Vandenberg, 1983), twelve poles from the Adige Embayment in the foreland of the Southern Alps (Márton et al., 2010, 2011), and eight poles from the Istria peninsula of Croatia (Márton et al., 2003, 2008) (Table 1). At six out of twelve localities from the Adige Embayment PSV is underrepresented ($A95 < A95_{min}$; Table 1). We assume that this is a result of within-sample averaging due to low sedimentation rates and have included these sites in our analysis.

Figure 7a shows all declinations vs. age, from all four sectors of Adria. Approximately 40 % of the poles are not statistically different from the expected African declinations. The remaining poles, representing the majority of the dataset, consistently show small counterclockwise deviations from the African APWP. The data provide no support for significant rotations between the northern and southern sectors of Adria.

To calculate the magnitude of rotation of Adria with respect to Africa we combine the data sets from the different regions. We used two approaches. One approach is to calculate a full-vector (six-point sliding window) moving average at every data point, from which we determined the D values and a ΔD error envelope. The other approach is to calculate a (fourth order) polynomial best-fit based on declination values only (Fig. 7b). Both approaches show a remarkably coincident pattern that display a systematic ccw deviation of the mean declination of Adria relative to Africa from the entire Early Cretaceous to Late Cenozoic time interval. We interpolated the declination curve of the APWP of Africa (Torsvik et al., 2012) to obtain the declination at the ages corresponding to our moving average, and determined the difference at each data point. This yields an average deviation of all data of $9.5 \pm 8.7^\circ$ ccw.

This obtained magnitude is accidentally comparable to the total rotation of Adria calculated from the upper Cretaceous of the Adige Embayment and Istria by Márton et al. (2010). These authors, however, interpreted their total rotation as the result of two distinct phases of cw and ccw rotation. In particular, an average of Eocene rocks was interpreted by Márton et al. (2010) to show 30° ccw rotation of Adria vs. Africa. They suggested a $\sim 20^\circ$ cw rotation of Adria between the Cretaceous and Eocene, followed by a post-Eocene $\sim 30^\circ$ ccw rotation. These Eocene poles are included in our analysis, but taking all available data into account, we see no solid ground for interpreting significant rotation phases between the early Cretaceous and the late Cenozoic.

In summary, paleomagnetic data allow for a counterclockwise rotation of Adria relative to Africa anywhere between negligible (1°) and quite significant (18°) values, but with a very consistent average of 9.5°. The timing of this rotation is ill constrained, but can be estimated from the average declination (Fig. 7) since roughly 20 ± 10 Ma.

SED
6, 937–983, 2014

4.2 Regional kinematic implications

The rotation pattern of Adria as emerging from this study can now be interpreted in the wider context of the central Mediterranean region. Our compilation of new and published paleomagnetic data do not lend support to models that infer either large Cretaceous vertical axis rotations (Dercourt et al., 1986; Márton et al., 2010) or a small cw rotation (Wortmann et al., 2007). We observe that two major types of scenarios can be accommodated within the range of rotation documented in this study (i.e. 1–18° ccw). One type of scenario is put forward from an Alpine point of view (post-20 Ma, $\sim 20°$ ccw rotation of Adria relative to Europe around an Euler pole in the western Alps, corresponding to a $\sim 17°$ ccw rotation of Adria relative to Africa). The other type derives from an Ionian Basin point of view (assuming near-rigidity between Africa and Adria and hence no differential rotation, according to Rosenbaum et al., 2004). The paleomagnetically permissible rotation range derived here, can therefore not discriminate the two end-member kinematic scenarios for Adria. Accordingly, we will show the kinematic consequences of the permitted minimum and maximum rotation of Adria as a function of the location of its Euler pole.

An Euler pole for the relative motion between Adria and Eurasia located at 45.0° N, 6°4 E, near the city of Torino was computed by Ustaszewski et al. (2008) based on westward decreasing Neogene shortening in the Alps, and northward underthrusting of Adria below the southern Alps. Their inferred 20° ccw rotation relative to Eurasia translates to a paleomagnetically permitted $\sim 17°$ ccw rotation of Adria relative to Africa. Assuming internal rigidity of Adria, a rotation around this pole by 17° would require up to 420 km of ENE–WSW extension in the Ionian Basin measured at the modern southeasternmost tip of stable Adria along the Kefallonia Fault (Fig. 8a). This scenario would require that the entire Ionian Basin is Miocene in age, inconsistent with any of the inferred ages that range from Permian to Cretaceous. Similarly, a 9.5° rotation of Adria (average rotation constrained by our paleomagnetic analysis) would yield ~ 230 km of ENE–WSW extension, still much higher than what is geologically documented (Fig. 8b).

SED
6, 937–983, 2014

Adria could rotate ccw without extension in the Ionian Basin if the Adria–Africa Euler pole is located in the far southeast of Adria (Fig. 8c). Assuming Adriatic rigidity, and applying the 17° ccw rotation derived from reconstructions of the Alps, this would, however, lead to a reconstructed overlap of (i.e. major Neogene extension between) Adria and the Dinarides and Hellenides, and predicts > 400 km of E–W convergence in the western Alps. Instead, Adria continuously converged with the Dinarides and Hellenides, and the amount of westward retreat of in the western Alps is much smaller than required by this scenario (e.g., Ustaszewski et al., 2008; van Hinsbergen and Schmid, 2012) (Fig. 8c).

Alternatively, we may explore the maximum amount of rotation around the Euler pole constrained by Ustaszewski et al. (2008) that is permitted by the available structural evidence from the Sicily Channel and kinematic reconstructions of the Aegean region, and that is comparable with the minimum permissible rotation documented by this study. The ~ 40 % crustal attenuation in the 140 km wide Sicily Channel (Civile et al., 2008) would suggest a (maximum) amount of NE–SW latest Miocene to Plio-Quaternary extension between Adria and Africa of ~ 40 km. A similar amount of Adria–Africa relative motion since the Early Pliocene was inferred to have occurred from a kinematic reconstruction of the Aegean region by van Hinsbergen and Schmid (2012) to avoid overlaps between Adria and the west-Aegean fold-thrust belt. This corresponds to a 1.7° ccw rotation of Adria. This reconstruction is consistent with the geological record of the circum-Ionian Basin, but it would require ~ 150 km NW–SE directed convergence between Adria and Europe since 20 Ma, to be accommodated in the Western Alps, in contrast with widely accepted lower values of no more than some tens of km (Ustaszewski et al., 2008; Handy et al., 2010) (Fig. 8d).

Our discussion above identifies a paradox between the kinematic interpretations from the geological record of the Alps and the Ionian Basin. Paleomagnetic data permit the scenarios that fulfill the constraints from both regions, but these scenarios cannot be reconciled with each other. Moreover, the average rotation suggested by the paleomagnetic data violates both end-member scenarios.

SED
6, 937–983, 2014

Since a key assumption in the above analysis is the rigidity of Adria, we explore a final scenario whereby we decouple north and south Adria, e.g. along the Mid-Adriatic Ridge, or along the Tremiti fault (Fig. 2). Applying the reconstruction of Ustaszewski et al. (2008) for North Adria (17° ccw rotation), and the reconstruction of van Hinsbergen and Schmid (2012) for South Adria (1.7° ccw rotation). This would require as much as 160 km of left-lateral strike-slip between North and South Adria, and none of the identified structures appear likely candidates to accommodate such major displacements (Fig. 8e).

The discussion above indicates that, although scenarios based on kinematic interpretations from both the Alps and the Ionian basin infer Neogene Adria–Africa relative rotations that are within the range documented in this study, these scenarios are mutually exclusive. Paleomagnetic data alone – with the error envelope calculated here – cannot solve this "Adriatic enigma", but calls for a reassessment of the kinematics of three areas centered around three questions: (i) since shortening reconstructions may underestimate the true amount of convergence: is the amount of Neogene shortening in the western Alps significantly underestimated? (ii) Is it possible to quantify the timing and amount of potential strike-slip zones separating a North and South Adria block? (iii) Is it possible that there is a large amount of Neogene extension along the Apulian escarpment, perhaps hidden below the advancing Calabrian prism and the Mediterranean ridge?

5 Conclusions

We provide six new paleomagnetic poles from the Lower Cretaceous to Upper Miocene of the Murge and Salento areas of the Apulian Platform, southern Italy. These new data, combined with recalculated published poles from the Gargano promontory, the Istria peninsula of Croatia, and the Adige Embayment of the southern Alps, constrain a counterclockwise rotation of Adria relative to Africa at $9.5 \pm 8.7°$, occurring sometime after 20 ± 10 Ma. Our revised paleomagnetic database for Adria discards significant ro-

SED
6, 937–983, 2014

tations of Adria vs. Africa between the Early Cretaceous and the Eocene, as invoked by several studies. The permissible rotation magnitude (1–18° counterclockwise) is consistent with two end-member models for the Central Mediterranean region requiring (i) a Neogene $\sim 18°$ counterclockwise rotation of Adria relative to Africa (based on kinematic reconstruction of the Alps), or (ii) negligible rotation of Adria based on kinematic reconstruction of the Ionian Basin. Although paleomagnetic data from Adria are not in disagreement with both models, we establish that these scenarios are mutually exclusive. We cannot solve this enigma, but call for kinematic studies focused on three key questions that may lead to a solution of the conundrum: (i) was Neogene shortening in the western Alps significantly underestimated? (ii) Was Neogene extension in the Ionian Basin significantly underestimated? (iii) Was a North Adria block decoupled from a South Adria block along a large-offset sinistral strike-slip fault?

Acknowledgements. Fieldwork was funded through the Netherlands research school of Integrated Solid Earth Sciences (ISES). DJJvH and MM were supported by ERC Starting Grant 306810 (SINK) and an NWO VIDI grant to DJJvH. LSa, LSp and MT were supported by Bari University funds (PRIN/COFIN 2009) grant to MT.

References

André, P. and Doulcet, A.: Rospo mare field – Italy, Apulian Platform, Adriatic Sea, in: Treatise of Petroleum Geology, Atlas of Oil and Gas Fields, Stratigraphic Traps II, edited by: Foster, N. H. and Beaumont, E. A., AAPG, Tulsa, 29–54, 1991.

Argnani, A.: The strait of sicily rift zone: foreland deformation related to the evolution of a backarc basin, J. Geodyn., 12, 311–331, 1990.

Argnani, A.: Evolution of the southern Tyrrhenian slab tear and active tectonics along the western edge of the Tyrrhenian subducted slab, Geol. Soc. Spec. Publ., 311, 193–212, 2009.

Argnani, A.: The influence of Mesozoic Palaeogeography on the variations in structural style along the front of the Albanide thrust-and-fold belt, IJG, 132, 175–185, 2013.

SED
6, 937–983, 2014

Argnani, A. and Bonazzi, C.: Malta Escarpment fault zone offshore eastern Sicily: Pliocene–Quaternary tectonic evolution based on new multichannel seismic data, Tectonics, 24, TC4009, doi:10.1029/2004TC001656, 2005.
Argnani, A., Favali, P., Frugoni, F., Gasperini, M., Ligi, M., Marani, M., Mattietti, G., and Mele, G.: Foreland deformational pattern in the Southern Adriatic Sea, Ann. Geofis., XXXVI, 229–247, 1993.
Argnani, A., Bonazzi, C., Evangelisti, D., Favali, P., Frugoni, F., Gasperini, M., Ligi, M., Marani, M., and Mele, G.: Tettonica dell'Adriatico meridionale, Mem. Soc. Geol. It., 51, 227–237, 1996.
Argnani, A., Frugoni, F., Cosi, R., Ligi, M., and Favali, P.: Tectonics and seismicity of the Apulian Ridge south of Salento peninsula (Southern Italy), Ann. Geophys.-Italy, 44, 527–540, 2001.
Belguith, Y., Geoffroy, L., Mourgues, R., and Rigane, A.: Analogue modelling of Late Miocene–Early Quaternary continental crustal extension in the Tunisia–Sicily Channel area, Tectonophysics, 608, 576–585, 2013.
Bernoulli, D. and Jenkyns, H. C.: Ancient oceans and continental margins of the Alpine–Mediterranean Tethys: deciphering clues from Mesozoic pelagic sediments and ophiolites, Sedimentology, 56, 149–190, 2009.
Bertotti, G., Picotti, V., Chilovi, C., Fantoni, R., Merlini, S., and Mosconi, A.: Neogene to Quaternary sedimentary basins in the south Adriatic (Central Mediterranean): foredeeps and lithospheric buckling, Tectonics, 20, 771–787, 2001.
Bonardi, G., Amore, F. O., Ciampo, G., and de Capoa, P.: Complesso Liguride Auct.: stato delle conoscenze e problemi aperti sulla sua evoluzione pre-appenninica ed i suoi rapporti con l'Arco Calabro, Memorie della Societa Geologica Italiana, 41, 17–35, 1988.
Bosellini, A.: Dinosaurs "re-write" the geodynamics of the eastern Mediterranean and the paleogeography of the Apulia Platform, Earth-Sci. Rev., 59, 211–234, 2002.
Bosellini, A., Bosellini, F. R., Colalongo, M. L., Parente, M., Russo, A., and Vescogni, A.: Statigraphic architecture of the Salento coast from Capo d'Otranto to S. Maria di Leuca (Apulia, southern Italy), Riv. Ital. Paleontol. S., 105, 397–416, 1999a.
Bosellini, A., Morsilli, M., and Neri, C.: Long-term event stratigraphy of the Apulia Platform margin (Upper Jurassic to Eocene, Gargano, southern Italy), J. Sediment. Res., 69, 1241–1252, 1999b.
Bosellini, F. R.: Biotic changes and their control on Oligocene–Miocene reefs: a case study from the Apulia Platform margin (southern Italy), Palaeogeogr. Palaeocl., 241, 393–409, 2006.

Bosellini, F. R. and Russo, A.: Stratigraphy and facies of an Oligocene fringing reef (Castro Limestone, Salento Peninsula, southern Italy), Facies, 26, 145–165, 1992.
Bosellini, F. R., Russo, A., and Vescogni, A.: Messinian reef-building assemblages of the Salento Peninsula (southern Italy): palaeobathymetric and palaeoclimatic significance, Palaeogeogr. Palaeocl., 175, 7–26, 2001.
Butler, R. F.: Paleomagnetism: Magnetic Domains to Geologic Terranes, Blackwell Scientific Publications, Boston, 1992.
Capitanio, F. A. and Goes, S.: Mesozoic spreading kinematics: consequences for Cenozoic Central and Western Mediterranean subduction, Geophys. J. Int., 165, 804–816, 2006.
Capitanio, F. A., Faccenna, C., Funiciello, R., and Salvini, F.: Recent tectonics of Tripolitania, Libya: an intraplate record of Mediterranean subduction, Geol. Soc. Spec. Publ., 357, 319–328, 2011.
Carminati, E., Lustrino, M., and Doglioni, C.: Tectonophysics, Tectonophysics, 579, 173–192, 2012.
Catalano, R., Doglioni, C., and Merlini, S.: On the mesozoic Ionian basin, Geophys. J. Int., 144, 49–64, 2001.
Cavazza, W., Ziegler, P. A., Spakman, W., and Stampfi, G.: The TRANSMED Atlas, Heidelberg, 2004.
Chamot-Rooke, N. and Rangin, C.: DOTMED – Deep Offshore Tectonics of the Mediterranean: a synthesis of deep marine data in eastern Mediterranean, Mem. S. Geo. F., 177, 1–64, 2005.
Channell, J.: Palaeomagnetism of limestones from the Gargano Peninsula (Italy), and the implication of these data, Geophys. J. Int., 51, 605–616, 1977.
Channell, J. and Tarling, D. H.: Palaeomagnetism and the rotation of Italy, Earth Planet. Sc. Lett., 25, 177–188, 1975.
Channell, J., D'Argenio, B., and Horvath, F.: Adria, the African promontory, in Mesozoic Mediterranean palaeogeography, Earth-Sci. Rev., 15, 213–292, 1979.
Ciaranfi, N., Pieri, P., and Ricchetti, G.: Note alla carta geologica delle Murge, Mem. Soc. Geol. It., 41, 449–460, 1988.
Cifelli, F., Mattei, M., and Rossetti, F.: Tectonic evolution of arcuate mountain belts on top of a retreating subduction slab: the example of the Calabrian Arc, J. Geophys. Res., 112, B09101, doi:10.1029/2006JB004848, 2007.

SED
6, 937–983, 2014

Did Adria rotate relative to Africa?

D. J. J. van Hinsbergen et al.

Civile, D., Lodolo, E., Tortorici, L., Lanzafame, G., and Brancolini, G.: Relationships between magmatism and tectonics in a continental rift: the Pantelleria Island region (Sicily Channel, Italy), Mar. Geol., 251, 32–46, 2008.

Civile, D., Lodolo, E., Accettella, D., and Geletti, R.: The Pantelleria graben (Sicily Channel, central Mediterranean): an example of intraplate "passive" rift, Tectonophysics, 490, 173–183, 2010.

Creer, K. M., Irving, A. J., and Nairn, A. E. M.: Paleomagnetism of the Great Whin Sill, Geophys. J. Roy. Astr. S., 2, 306–323, 1959.

D'Agostino, N., Avallone, A., Cheloni, D., D'Anastasio, E., Mantenuto, S., and Selvaggi, G.: Active tectonics of the Adriatic region from GPS and earthquake slip vectors, J. Geophys. Res., 113, B12413, doi:10.1029/2008JB005860, 2008.

D'Argenio, B., Pescatore, T., and Scandone, P.: Schema geologico dell'Appennino meridionale (Campania e Lucania), Accademia Nazionale dei Lincei, 183, 49–72, 1973.

de Alteriis, G.: Different foreland basins in Italy: examples from the central and southern Adriatic Sea, Tectonophysics, 252, 349–373, 1995.

Deenen, M. H. L., Langereis, C. G., van Hinsbergen, D. J. J., and Biggin, A. J.: Geomagnetic secular variation and the statistics of palaeomagnetic directions, Geophys. J. Int., 186, 509–520, 2011.

Del Ben, A., Geletti, R., and Mocnik, A.: Relation between recent tectonics and inherited Mesozoic structures of the central-southern Adria plate, B. Geofis. Teor. Appl., 51, 99–115, 2010.

Dercourt, J., Zonenshain, L. P., Ricou, L. E., and Kazmin, V. G.: Geological evolution of the Tethys belt from the Atlantic to the Pamirs since the Lias, Tectonophysics, 123, 241–315, 1986.

Dercourt, J., Gaetani, M., Vrielynck, B., Barrier, E., Biju-Duval, B., Brunet, M. F., Cadet, J. P., Crasquin, S., and Sandulescu, M.: Atlas Peri-Tethys, palaeogeographical maps, CCGM/CGMW, Paris, 2000.

Dewey, J. F. and Sengör, A. M. C.: Aegean and surrounding regions: complex multiplate and continuum tectonics in a convergent zone, Geol. Soc. Am. Bull., 90, 84–92, 1979.

Dewey, J. F., Helman, M. L., Knott, S. D., Turco, E., and Hutton, D. H. W.: Kinematics of the western Mediterranean, Geol. Soc. Spec. Publ., 45, 265–283, 1989.

Doglioni, C.: A proposal for the kinematic modelling of W-dipping subductions – possible applications to the Tyrrhenian–Apennines system, Terra Nova, 3, 423–434, 1991.

SED
6, 937–983, 2014

Did Adria rotate relative to Africa?

D. J. J. van Hinsbergen et al.

Doglioni, C., Mongelli, F., and Pieri, P.: The Puglia uplift (SE Italy): an anomaly in the foreland of the Apenninic subduction due to buckling of a thick continental lithosphere, Tectonics, 13, 1309–1321, 1994.
Doglioni, C., Gueguen, E., Sabàt, F., and Fernandez, M.: The Western Mediterranean extensional basins and the Alpine orogen, Terra Nova, 9, 109–112, 1997.
Faccenna, C. and Becker, T. W.: Shaping mobile belts by small-scale convection, Nature, 465, 602–605, 2010.
Faccenna, C., Funiciello, F., Giardini, D., and Lucente, P.: Episodic back-arc extension during restricted mantle convection in the Central Mediterranean, Earth Planet. Sc. Lett., 187, 105–116, 2001.
Faccenna, C., Piromallo, C., Crespo-Blanc, A., Jolivet, L., and Rossetti, F.: Lateral slab deformation and the origin of the western Mediterranean arcs, Tectonics, 23, TC1012, doi:10.1029/2002TC001488, 2004.
Fantoni, R. and Franciosi, R.: Tectono-sedimentary setting of the Po Plain and Adriatic foreland, Rend. Fis. Acc. Lincei, 21, 197–209, 2010.
Favali, P., Mele, G., and Mattietti, G.: Contribution to the study of the Apulian microplate geodynamics, Mem. Soc. Geol. It., 44, 71–80, 1990.
Favali, P., Funiciello, R., Mattietti, G., Mele, G., and Salvini, F.: An active margin across the Adriatic Sea (central Mediterranean Sea), Tectonophysics, 219, 109–117, 1993.
Favre, P. and Stampfli, G. M.: From rifting to passive margin: the examples of the Red Sea, Central Atlantic and Alpine Tethys, Tectonophysics, 215, 69–97, 1992.
Festa, V.: Cretaceous structural features of the Murge area (Apulian Foreland, Southern Italy), Eclogae Geol. Helv., 96, 11–22, 2003.
Festa, V., Teofilo, G., Tropeano, M., and Sabato, L.: New insights on diapirism in the Adriatic Sea: the Tremiti salt structure (Apulia offshore, southeastern Italy), Terra Nova, in press, doi:10.1111/ter.12082, 2014.
Finetti, I.: Structure, stratigraphy and evolution of the central Mediterranean Sea, B. Geofis. Teor. Appl., 24, 247–312, 1982.
Finetti, I.: Structure and Evolution of the Central Mediterranean (Pelagian and Ionian Seas), Springer, New York, NY, 215–230, 1985.
Fisher, R. A.: Dispersion on a sphere, P. R. Soc. London, A217, 295–305, 1953.
Flores, G., Pieri, M., and Sestini, G.: Geodynamic history and petroleum habitats of the southeast Adriatic region, AAPG Special Publication, 1, 389–398, 1991.

Frisch, W.: Tectonic progradation and plate tectonic evolution of the Alps, Tectonophysics, 60, 121–139, 1979.
Frizon de Lamotte, D., Raulin, C., Mouchot, N., Wrobel-Daveau, J.-C., Blanpied, C., and Ringenbach, J.-C.: The southernmost margin of the Tethys realm during the Mesozoic and Cenozoic: initial geometry and timing of the inversion processes, Tectonics, 30, TC3002, doi:10.1029/2010TC002691, 2011.
Gaina, C., Roest, W. R., and Müller, R. D.: Late Cretaceous–Cenozoic deformation of northeast Asia, Earth Planet. Sc. Lett., 197, 273–286, 2002.
Gaina, C., Torsvik, T. H., van Hinsbergen, D. J. J., Medvedev, S., Werner, S. C., and Labails, C.: The African Plate: a history of oceanic crust accretion and subduction since the Jurassic, Tectonophysics, 604, 4–25, 2013.
Gallais, F., Gutscher, M.-A., Graindorge, D., Chamot-Rooke, N., and Klaeschen, D.: A Miocene tectonic inversion in the Ionian Sea (central Mediterranean): evidence from multichannel seismic data, J. Geophys. Res., 116, B12108, doi:10.1029/2011JB008505, 2011.
Gambini, R. and Tozzi, M.: Tertiary geodynamic evolution of the Southern Adria microplate, Terra Nova, 8, 593–602, 1996.
Goes, S., Giardini, D., Jenny, S., Hollenstein, C., Kahle, H. G., and Geiger, A.: A recent tectonic reorganization in the south-central Mediterranean, Earth Planet. Sc. Lett., 226, 335–345, 2004.
Golonka, J.: Plate tectonic evolution of the southern margin of Eurasia in the Mesozoic and Cenozoic, Tectonophysics, 381, 235–273, 2004.
Govers, R. and Wortel, M. J. R.: Lithosphere tearing at STEP faults: response to edges of subduction zones, Earth Planet. Sc. Lett., 236, 505–523, 2005.
Gradstein, F. M., Ogg, J. G., Schmitz, M., and Ogg, G.: The Geologic Time Scale 2012, Elsevier, Amsterdam, 2012.
Grandic, S., Biancone, M., and Samarzija, J.: Geophysical and stratigraphic evidence of the Triassic rift structuration in the Adriatic offshore area, Mem. Soc. Geol. It., 57, 315–325, 2002.
Gueguen, E., Doglioni, C., and Fernandez, M.: On the post-25 Ma geodynamic evolution of the western Mediterranean, Tectonophysics, 298, 259–269, 1998.
Handy, M. R., Schmid, S. M., Bousquet, R., Kissling, E., and Bernoulli, D.: Earth-Sci. Rev., 102, 121–158, 2010.

SED
6, 937–983, 2014

Did Adria rotate relative to Africa?

D. J. J. van Hinsbergen et al.

Hieke, W., Cita, M. B., and Forcella, F.: Geology of the Victor Hensen Seahill (Ionian Sea, eastern Mediterranean); insights from the study of cored sediment sequences, B. Soc. Geol. Ital., 125, 245–257, 2006.

Iannone, A. and Laviano, A.: Studio stratigrafico e paleoambientale di una successione cenomaniano-turoniana (Calcare di Bari) affiorante presso Ruvo di Puglia, Geologica Romana, 19, 209–230, 1980.

Johnson, C. L., Constable, C. G., Tauxe, L., Barendregt, R., Brown, L. L., Coe, R. S., Layer, P., Mejia, V., Opdyke, N. D., Singer, B. S., Staudigel, H., and Stone, D. B.: Recent investigations of the 0–5 Ma geomagnetic field recorded by lava flows, Geochem. Geophy. Geosy., 9, Q04032, doi:10.1029/2007GC001696, 2008.

Jolivet, L., Faccenna, C., and Piromallo, C.: From mantle to crust: stretching the Mediterranean, Earth Planet. Sc. Lett., 285, 198–209, 2009.

Kastelic, V., Vannoli, P., Burrato, P., Fracassi, U., Tiberti, M. M., and Valensise, G.: Marine and Petroleum Geology, Mar. Petrol. Geol., 42, 191–213, 2013.

Kirschvink, J. L.: The least-squares line and plane and the analysis of palaeomagnetic data, Geophys. J. Roy. Astr. S., 62, 699–718, 1980.

Kokkalas, S., Kamberis, E., Xypolias, P., and Sotiropoulos, S.: Coexistence of thin-and thick-skinned tectonics in Zakynthos area (western Greece): insights from seismic sections and regional seismicity, Tectonophysics, 597/598, 73–84, 2013.

Laviano, A., Maresca, M. G., and Tropeano, M.: Stratigraphic organization of rudist biogenic beds in the Upper Cenomanian successions of the Western Murge (Apulia, Southern Italy), Geobios-Lyon, 31, 159–168, 1998.

Luperto-Sinni, E. and Borgomano, J.: Le Crétacé supérieur des Murges sud-orientales (Italie méridionale): stratigraphie et évolution des paléoenvironnements, Riv. Ital. Paleontol. S., 95, 95–136, 1989.

Luperto-Sinni, E. and Masse, J.-P.: Données nouvelles sur la micropaléontologie et la stratigraphie de la partie basale du “Calcare di Bari” (Crétacé inférieur) dans la région des Murges (Italie méridionale), Riv. Ital. Paleontol. S., 90, 331–374, 1984.

Malinverno, A. and Ryan, W. B. F.: Extension in the Tyrrhenian Sea and shortening in the Apennines as result of arc migration driven by sinking of the lithosphere, Tectonics, 5, 227–245, 1986.

Márton, E. and Nardi, G.: Cretaceous palaeomagnetic results from Murge (Apulia, southern Italy): tectonic implications, Geophys. J. Int., 119, 842–856, 1994.

Márton, E., Drobne, J., Ćosović, V., and Moro, A.: Palaeomagnetic evidence for Tertiary counterclockwise rotation of Adria, Tectonophysics, 377, 143–156, doi:10.1016/j.tecto.2003.08.022, 2003.
Márton, E., Ćosović, V., Moro, A., and Zvocak, S.: The motion of Adria during the Late jurassic and Cretacous: new paleomagnetic results from stable Istria, Tectonophysics, 454, 44–53, 2008.
Márton, E., Zampieri, D., Grandesso, P., Ćosović, V., and Moro, A.: New Cretaceous paleomagnetic results from the foreland of the Southern Alps and the refined apparent polar wander path for stable Adria, Tectonophysics, 480, 57–72, 2010.
Márton, E., Zampieri, D., Kázmér, M., Dunkl, I., and Frisch, W.: New Paleocene–Eocene paleomagnetic results from the foreland of the Southern Alps confirm decoupling of stable Adria from the African plate, Tectonophysics, 504, 89–99, 2011.
Mastrogiacomo, G., Moretti, M., Owen, G., and Spalluto, L.: Tectonic triggering of slump sheets in the Upper Cretaceous carbonate succession of the Porto Selvaggio area (Salento peninsula, southern Italy): synsedimentary tectonics in the Apulian Carbonate Platform, Sediment. Geol., 269, 15–27, 2012.
Mattavelli, L., Novelli, L., and Anelli, L.: Occurrence of hydrocarbons in the Adriatic basin, AAPG Special Publication, 1, 369–380, 1991.
McFadden, P. C. and McElhinny, M. W.: Classification of the reversal test in palaeomagnetism, Geophys. J. Int., 103, 725–729, 1990.
Minelli, L. and Faccenna, C.: Evolution of the Calabrian accretionary wedge (central Mediterranean), Tectonics, 29, TC4004, doi:10.1029/2009TC002562, 2010.
Mullender, T. A. T., Van Velzen, A. J., and Dekkers, M. J.: Continuous drift correction and separate identification of ferrimagnetic and paramagnetic contribution in thermamagnetic runs, Geophys. J. Int., 114, 663–672, 1993.
Müller, R. D., Royer, J.-Y., Cande, S. C., Roest, W. R., and Maschenkov, S.: New constraints on the Late Cretaceous/Tertiary plate tectonic evolution of the Caribbean, Sedimentary Basins of the World, 4, 33–59, 1999.
Oldow, J. S., Ferranti, L., D'Argenio, B., Catalano, R., and Pappone, G.: Active fragmentation of Adria, the north African promontory, Central Mediterranean Orogen„ 30, 779–774, 2002.
Parente, M.: A revised stratigraphy of the Upper Cretaceous to Oligocene units from southeastern Salento (Apulia, southern Italy), Boll. Soc. Paleontol. I., 33, 155–170, 1994.

Pasquale, V., Verdoya, M., and Chiozzi, P.: Thermal Structure of the Ionian Slab, Pure Appl. Geophys., 162, 967–986, 2005.

Picha, F. J.: Late orogenic strike-slip faulting and escape tectonics in frontal Dinarides-Hellenides, Croatia, Yugoslavia, Albania, and Greece, AAPG Bull., 86, 1659–1671, 2002.

Pieri, P. and Laviano, A.: Tettonica e sedimentazione nei depositi senoniani delle Murge sud-orientali (Ostuni), B. Soc. Geol. Ital., 108, 351–356, 1989.

Pieri, P., Festa, V., Moretti, M., and Tropeano, M.: Quaternary tectonic activity of the Murge area (Apulian foreland – Southern Italy), Ann. Geophys.-Italy, 40, 1395–1404, doi:10.4401/ag-3876, 1997.

Reina, A. and Luperto-Sinni, E.: Contributo alla conoscenza stratigrafica del Cretaceo superiore in facies di piattaforma carbonatica interna del Salento occidentale (Puglia, Italia meridionale), B. Soc. Geol. Ital., 33, 145–153, 1994a.

Reina, A. and Luperto-Sinni, E.: Le Dolomie di Monte, S. Elia: proposta per una nuova unità formazionale del Cretaceo delle Murge (Puglia, Italia meridionale), Paleopelagos, 4, 233–241, 1994b.

Reston, T. J., von Huene, R., Dickmann, R., Klaeschen, D., and Kopp, H.: Frontal accretion along the western Mediterranean Ridge: the effect of Messinian evaporites on wedge mechanics and structural style, Mar. Geol., 186, 59–82, 2002.

Ricchetti, G.: Nuovi dati stratigrafici sul Cretaceo delle Murge emersi da indagini nel sottosuolo, B. Soc. Geol. Ital., 94, 1083–1108, 1975.

Ricchetti, G., Ciaranfi, N., Luperto-Sinni, E., Mongelli, F., and Pieri, P.: Geodinamica ed evoluzione sedimentaria e tettonica dell'avampaese apulo, Mem. Soc. Geol. It., 41, 57–82, 1998.

Robertson, A. H. F., Clift, P. D., Degnan, P. J., and Jones, G.: Palaeogeographic and palaeotectonic evolution of the Eastern Mediterranean Neotethys, Palaeogeogr. Palaeocl., 87, 289–343, 1991.

Rosenbaum, G. and Lister, G. S.: Formation of arcuate orogenic belts in the western Mediterranean region, Orogenic curvature: integrating paleomagnetic and structural analyses, 41–56, 2004.

Rosenbaum, G. and Lister, G. S.: The Western Alps from the Jurassic to Oligocene: spatio-temporal constraints and evolutionary reconstructions, Earth-Sci. Rev., 69, 281–306, 2005.

Rosenbaum, G., Lister, G. S., and Duboz, C.: Relative motions of Africa, Iberia and Europe during Alpine orogeny, Tectonophysics, 359, 117–129, 2002.

Rosenbaum, G., Lister, G. S., and Duboz, C.: The Mesozoic and Cenozoic motion of Adria (central Mediterranean): a review of constraints and limitations, Geodin. Acta, 17, 125–139, 2004.
Rosenbaum, G., Gasparon, M., Lucente, F. P., Peccerillo, A., and Miller, M. S.: Kinematics of slab tear faults during subduction segmentation and implications for Italian magmatism, Tectonics, 27, TC2008, doi:10.1029/2007TC002143, 2008.
Royden, L. H. and Papanikolaou, D. J.: Slab segmentation and late Cenozoic disruption of the Hellenic arc, Geochem. Geophy. Geosy., 12, Q03010, doi:10.1029/2010GC003280, 2011.
Savostin, L. A., Sibuet, J. C., Zonenshain, L. P., Le Pichon, X., and Roulet, M.-J.: Kinematic evolution of the Tethys belt from the Atlantic Ocean to the Pamirs since the Triassic, Tectonophysics, 123, 1–35, 1986.
Scheepers, P.: No tectonic rotation for the Apulia-Gargano foreland in the Pleistocene, Geophys. Res. Lett., 19, 2275–2278, 1992.
Schettino, A. and Turco, E.: Tectonic history of the western Tethys since the Late Triassic, Geol. Soc. Am. Bull., 123, 89–105, 2011.
Schmid, S. M., Bernoulli, D., Fügenschuh, B., Maþenco, L., Schefer, S., Schuster, R., Tischler, M., and Ustaszewski, K.: The Alpine–Carpathian–Dinaridic orogenic system: correlation and evolution of tectonic units, Swiss J. Geosci., 101, 139–183, 2008.
Schmid, S. M., Scharf, A., Handy, M. R., and Rosenberg, C. L.: The Tauern Window (Eastern Alps, Austria): a new tectonic map, with cross-sections and a tectonometamorphic synthesis, Swiss J. Geosci., 106, 1–32, 2013.
Schönborn, G.: Balancing cross sections with kinematic constraints: the Dolomites (northern Italy), Tectonics, 18, 527–545, 1999.
Scisciani, V. and Calamita, F.: Active intraplate deformation within Adria: examples from the Adriatic region, Tectonophysics, 476, 57–72, 2009.
Scrocca, D.: Thrust front segmentation induced by differential slab retreat in the Apennines (Italy), Terra Nova, 18, 154–161, 2006.
Sengör, A. M. C., Yilmaz, Y., and Sungurlu, O.: Tectonics of the Mediterranean Cimmerides: nature and evolution of the western termination of Palaeo-Tethys, Geol. Soc. Spec. Publ., 17, 77–112, 1984.
Seton, M., Müller, R. D., Zahirovic, S., Gaina, C., Torsvik, T. H., Shephard, G., Talsma, A., Gurnis, M., Turner, M., Maus, S., and Chandler, M.: Global continental and ocean basin reconstructions since 200 Ma, Earth-Sci. Rev., 113, 212–270, 2012.

Spalluto, L.: Facies evolution and sequence chronostratigraphy of a “mid-”Cretaceous shallow-water carbonate succession of the Apulia Carbonate Platform from the northern Murge area (Apulia, southern Italy), Facies, 58, 17–36, 2011.

Spalluto, L. and Caffau, M.: Stratigraphy of the mid-Cretaceous shallow-water limestones of the Apulia Carbonate Platform (Murge, Apulia, southern Italy), IJG, 129, 335–352, 2010.

Spalluto, L., Pieri, P., and Ricchetti, G.: Le facies carbonatiche di piattaforma interna del Promontorio del Gargano; implicazioni paleoambientali e correlazioni con la coeva successione delle Murge (Italia meridionale, Puglia), IJG, 124, 675–690, 2005.

Speranza, F. and Kissel, C.: First paleomagnetism of eocene rocks from Gargano: widespread overprint or non rotation?, Geophys. Res. Lett., 20, 2627–2630, 1993.

Speranza, F., Minelli, L., Pignatelli, A., and Chiappini, M.: The Ionian Sea: the oldest in situ ocean fragment of the world?, J. Geophys. Res., 117, B12101, doi:10.1029/2012JB009475, 2012.

Stampfli, G. M. and Borel, G. D.: A plate tectonic model for the Paleozoic and Mesozoic constrained by dynamic plate boundaries and restored synthetic oceanic isochrons, Earth Planet. Sc. Lett., 196, 17–33, 2002.

Stampfli, G. M. and Hochard, C., Eds.: Plate tectonics of the Alpine realm, Geol. Soc. Spec. Publ., 327, 89–111, 2009.

Stampfli, G. M. and Mosar, J.: The making and becoming of Apulia, Mem. Sci. Geol., 51, 141–154, 1999.

Tauxe, L. and Kent, D. V.: A simplified statistical model for the geomagnetic field and the detection of shallow bias in paleomagnetic inclinations: was the ancient magnetic field dipolar? Timescales of the Paleomagnetic field, Geoph. Monog. Series, 145, 101–115, 2004.

Torsvik, T. H., Van der Voo, R., Preeden, U., Mac Niocaill, C., Steinberger, B., Doubrovine, P. V., van Hinsbergen, D. J. J., Domeier, M., Gaina, C., Tohver, E., Meert, J. G., McCausland, P. J. A., and Cocks, L. R. M.: Phanerozoic polar wander, paleogeography and dynamics, Earth-Sci. Rev., 114, 325–368, 2012.

Tozzi, M., Kissel, C., Funiciello, R., Laj, C., and Parotto, M.: A clockwise rotation of southern Apulia?, Geophys. Res. Lett., 15, 681–684, 1988.

Tropeano, M., Spalluto, L., Moretti, M., Pieri, P., and Sabato, L.: Depositi carbonatici infrapleistocenici di tipo Foramol in sestemi di scarpata (Salento-Italia Meridionale), Il Quaternario, 17, 537–546, 2004.

Underhill, J. R.: Late Cenozoic deformation of the Hellenide foreland, western Greece, Geol. Soc. Am. Bull., 101, 613–634, 1989.
Ustaszewski, K., Schmid, S. M., Fügenschuh, B., Tischler, M., Kissling, E., and Spakman, W.: A map-view restoration of the Alpine–Carpathian–Dinaridic system for the Early Miocene, Swiss J. Geosci., 101, 273–294, 2008.
Vai, G. B. and Martini, I. P.: Anatomy of an Orogen: the Apennines and Adjacent Mediterranean Basins, Springer, Dordrecht, 637 pp., 2001.
van Hinsbergen, D. J. J. and Schmid, S. M.: Map view restoration of Aegean–West Anatolian accretion and extension since the Eocene, Tectonics, 31, TC5005, doi:10.1029/2012TC003132, 2012.
van Hinsbergen, D. J. J., van der Meer, D. G., Zachariasse, W. J., and Meulenkamp, J. E.: Deformation of western Greece during Neogene clockwise rotation and collision with Apulia, Int. J. Earth Sci., 95, 463–490, 2006.
van Hinsbergen, D. J. J., Vissers, R. L. M., and Spakman, W.: Origin and consequences of western Mediterranean subduction, rollback, and slab segmentation, Tectonics, 33, in press, doi:10.1002/2013TC003349, 2014.
Vandenberg, J.: Reappraisal of paleomagnetic data from Gargano (South Italy), Tectonophysics, 98, 29–41, 1983.
Vescogni, A.: Evoluzione delle biocostruzioni a vermetidi e loro utilizzo come "markers" paleobatimetrici e paleoclimatici, Giornale di Geologia, 62, 55–61, 2000.
Vissers, R., van Hinsbergen, D. J. J., Meijer, P. T., and Piccardo, G.: Kinematics of Jurassic ultra-slow spreading in the Piemonte Ligurian ocean, Earth Planet. Sc. Lett., 380, 138–150, 2013.
Vlahoviæ, I., Tišljar, J., Veliæ, I., and Matièec, D.: Evolution of the Adriatic Carbonate Platform: palaeogeography, main events and depositional dynamics, Palaeogeography, 220, 333–360, 2005.
Wortel, M. J. R. and Spakman, W.: Subduction and slab detachment in the Mediterranean–Carpathian region, Science, 290, 1910–1917, 2000.
Wortmann, U. G., Weissert, H., Funk, H., and Hauck, J.: Alpine plate kinematics revisited: the Adria Problem, Tectonics, 20, 134–147, 2007.
Zappaterra, E.: Carbonate paleogeographic sequences of the peradriatic region, B. Soc. Geol. Ital., 109, 5–20, 1990.

Zappaterra, E.: Source–rock distribution model of the Periadriatic Region, AAPG Bull., 78, 333–354, 1994.
Zijderveld, J. D. A.: A. C. demagnetization of rocks: analysis of results, in: Methods in Palaeomagnetism, Elsevier, Amsterdam, New York, 254–286, 1967.

SED
6, 937–983, 2014

Did Adria rotate relative to Africa?

D. J. J. van Hinsbergen et al.

Table 1a. Table showing all the data of our, and published paleomagnetic results for Adria. Areas are indicated in Fig. 1. Lat = Latitude of the site; Lon = Longitude of the site; Ages are assigned based on the biostratigraphy of the sites, and translated into numerical ages using Gradstein et al. (2012); N_d = number of demagnetized specimens; N_i = number of interpreted specimens; N45 = total number of specimens that fall within the 45° cut-off; D = declination; ΔDx = error on declination sensu Butler (1992); I = Inclination; ΔIx = error in inclination sensu Butler (1992). Statistical parameters are given by a cone confidence using Fisher (1953) statistics on virtual geomagnetic poles (A95, K) and directions (α95, k). A95$_{min}$ and A95$_{max}$ correspond to the confidence envelope of Deenen et al. (2011). Right-hand panel: directions and errors at a reference location 40.7° N, 17.2° E.

code	site name	source	area	lat	lon	Age	ΔAge	N_d/N_i	N45	D	ΔD	I	ΔI
MN	MN1 (Novaglie Lower Messinian)	This study	Apulia	39.9	18.4	6.6	0.6	20/16	14	355.1	12.5	61.1	7.8
	MN3 (Novaglie Lower Messinian)	This study	Apulia	39.9	18.4	6.6	0.6	20/13	8	42.5	13.7	33.2	20.2
OC	OC (Oligocene Castro)	This study	Apulia	40.0	18.4	25.6	2.6	45/31	29	0.5	3.2	44.2	3.7
TS	TS (Torre Specchialaguardia)	This study	Apulia	40.0	18.5	35.9	2.0	56/55	47	356.0	5.7	44.8	6.4
	MA (Massafra Quarry)	This study	Apulia	40.6	17.1	69.1	3.1	40/18	17	8.8	10.6	46.6	11.4
	CN (Caranna Quarry)	This study	Apulia	40.8	17.4	72.1	4.0	45/15	15	2.3	11.7	51.7	10.7
PS	PS (Porto Selvaggio Cove)	This study	Apulia	40.2	18.0	74.0	2.0	53/14	14	345.0	8.9	18.4	16.3
CU	CU (Cavallarizza Quarry)	This study	Apulia	41.0	16.4	95.6	1.7	50/43	32	333.2	7.2	44.9	8.0
PA	PA (Petraro Quarry)	This study	Apulia	41.3	16.3	138.0	2.0	48/39	29	310.8	8.5	23.4	14.6
1	Upper Plio–Pleistocene	Scheepers (1992)	Apulia	40.5	16.5	2.7	0.9		40	0.9	3.9	55.7	3.0
2	Pliocene–Quaternary (in situ)	Tozzi et al. (1988)	Apulia	40.0	18.4	3.2	2.2		30	0.9	2.2	64.6	59.7
3	Miocene (in situ)	Tozzi et al. (1988)	Apulia	40.0	18.4	14.2	8.8		20	351.6	8.9	56.6	37.3
4	Eocene/Oligocene (in situ)	Tozzi et al. (1988)	Apulia	40.0	18.4	26.8	1.3		93	356.5	1.3	46.9	185.7
5	Conamanian–Turonian	Márton and Nardi (1994)	Apulia	41.0	16.3	95.1	2.1		30	333.1	2.4	36.2	59.7
6	Lower–Middle Cenomanian	Márton and Nardi (1994)	Apulia	41.0	16.3	98.9	1.6		26	314.9	2.3	45.3	51.8
7	Middle Eocene	Speranza and Kissel (1993)	Gargano	41.8	16.1	44.5	3.3		114	352.0	3.3	46.7	225.7
8	Turonian–Senonian	Van den Berg et al. (1993)	Gargano	41.9	16.0	83.0	10.9		123	326.1	13.2	46.0	212.9
9	Turonian	Channel and Tarling (1975)	Gargano	41.7	15.7	90.1	3.8		39	334.0	4.2	36.3	76.7
10	Turonian–Coniacian	Channel et al. (1977)	Gargano	41.9	16.0	91.9	2.0		114	335.1	2.2	35.7	227.0
11	Neocomian–Aptian	Van den Berg et al. (1993)	Gargano	41.9	16.0	124.0	15.4		47	315.3	21.9	41.2	66.3
12	Priabonian	Márton et al. (2011)	Adige	45.6	11.4	35.9	2.0		37	6.2	9.7	64.1	5.3
13	Lutetian	Márton et al. (2011)	Adige	45.3	11.7	44.5	3.3		15	336.2	7.4	51.1	6.9
14	Ypresian	Márton et al. (2011)	Adige	45.4	11.5	51.9	4.1		49	332.9	4.9	46.3	5.2
15	Paleocene	Márton et al. (2011)	Adige	45.6	11.3	61.0	5.0		17	348.1	3.5	36.6	4.9
16	Maastrichtian	Márton et al. (2010)	Adige	45.5	11.3	69.1	3.1		13	337.1	3.0	32.1	4.5
17	Campanian	Márton et al. (2010)	Adige	45.5	11.3	77.9	5.8		29	336.8	2.3	43.4	2.7
18	Upper Coniacian	Márton et al. (2010)	Adige	45.5	11.3	87.2	0.9		40	336.5	2.9	44.2	3.3
19	Coniacian	Márton et al. (2010)	Adige	45.5	11.3	88.1	1.8		34	331.8	3.7	37.5	5.0
20	Turonian–Coniacian	Márton et al. (2010)	Adige	45.5	11.3	90.1	3.8		44	328.9	2.2	38.7	2.9
21	Cenomanian	Márton et al. (2010)	Adige	45.5	11.3	97.2	3.3		46	330.1	3.3	37.3	4.5
22	Valanginian–Hauterivian	Márton et al. (2010)	Adige	45.5	11.3	135.1	4.3		39	305.8	5.3	42.7	6.3
23	Berriasian	Márton et al. (2010)	Adige	45.5	11.3	142.2	2.8		17	302.4	3.5	41.3	4.3
24	Lutetian	Márton et al. (2003)	Istria	45.3	13.9	44.5	3.3		35	337.1	8.5	53.1	7.4
25	Cuisian	Márton et al. (2003)	Istria	45.3	13.9	46.0	8.0		29	342.8	9.4	48.5	9.4
26	Turonian–Coniacian	Márton et al. (2008)	Istria	45.1	13.7	90.1	3.8		42	332.7	7.0	55.4	5.6
27	Turonian	Márton et al. (2008)	Istria	45.1	13.7	91.9	2.1		33	340.4	4.1	48.6	4.1
28	Cenomanian	Márton et al. (2008)	Istria	45.1	13.7	97.2	3.3		49	346.3	10.4	61.0	6.6
29	Albian	Márton et al. (2008)	Istria	45.1	13.7	106.8	6.3		64	330.3	3.5	42.5	4.2
30	Valanginian–Aptian	Márton et al. (2008)	Istria	45.1	13.7	126.2	13.2		29	316.3	6.7	43.5	7.8
31	Tithonian	Márton et al. (2008)	Istria	45.1	13.7	148.6	3.5		17	314.9	4.4	47.3	4.6

SED
6, 937–983, 2014

Table 1b. Continued.

code	site name	source	A95	A95$_{min}$	A95$_{max}$	K	(α95)	(k)	λp	ϕp	reference location 40.7° N/17.2° E D(ref)	ΔD(ref)	I(ref)	ΔI(ref)
MN	MN1 (Novaglie Lower Messinian)	This study	9.2	4.2	15.6	19.5	6.9	34.3	85.7	255.0	355.3	11.8	57.6	8.6
	MN3 (Novaglie Lower Messinian)	This study	13.0	5.2	22.1	19.0	14.9	14.7	47.5	126.5				
OC	OC (Oligocene Castro)	This study	2.9	3.1	9.8	85.8	3.1	75.6	75.9	196.6	0.2	3.2	45.1	3.6
TS	TS (Torre Specchialaguardia)	This study	5.1	2.6	7.3	17.9	5.1	17.7	76.0	213.4	355.6	5.7	45.7	6.3
	MA (Massafra Quarry)	This study	9.4	3.9	13.8	15.2	10.2	13.1	75.3	164.9				
	CN (Caranna Quarry)	This study	9.9	4.1	14.9	15.7	8.3	22.0	81.4	184.4				
PS	PS (Porto Selvaggio Cove)	This study	8.8	4.2	15.6	11.0	11.9	12.1	56.5	225.5	344.6	8.9	19.7	16.1
CU	CU (Cavallarizza Quarry)	This study	6.4	3.0	9.2	16.8	7.2	13.4	63.6	261.5	333.5	7.1	44.2	8.1
PA	PA (Petraro Quarry)	This study	*8.3*	3.1	9.8	11.5	9.1	9.6	38.3	266.8	311.4	8.5	22.1	14.8
1	Upper Plio–Pleistocene	Scheepers (1992)	*3.1*	*2.7*	*8.0*	*54.1*	2.7	71.8	85.7	186.8	1.0	3.9	55.9	3.0
2	Pliocene–Quaternary (in situ)	Tozzi et al. (1988)	*4.0*	*3.1*	*9.6*	*44.3*	2.7	94.3	83.5	192.9	0.6	4.8	53.7	4.1
3	Miocene (in situ)	Tozzi et al. (1988)	*4.3*	*3.6*	*12.4*	*57.5*	3.9	72.6	82.9	267.8	351.4	5.5	57.4	4.0
4	Eocene/Oligocene (in situ)	Tozzi et al. (1988)	*3.3*	*2.0*	*4.7*	*20.8*	3.2	21.9	77.8	213.1	356.2	3.8	47.8	3.9
5	Conamanian–Turonian	Márton and Nardi (1994)	*3.1*	*3.1*	*9.6*	*72.7*	3.3	65.6	59.0	252.0	333.5	3.3	35.3	4.6
6	Lower–Middle Cenomanian	Márton and Nardi (1994)	*6.4*	*3.3*	*10.5*	*20.9*	6.2	21.9	50.5	279.9	315.4	7.1	44.4	8.1
7	Middle Eocene	Speranza and Kissel (1993)	*2.4*	*1.8*	*4.1*	*26.7*	2.4	32.6	74.7	223.9	352.4	2.9	45.2	3.2
8	Turonian–Senonian	Van den Berg et al. (1993)	*2.1*	*1.8*	*4.0*	*36.2*	2.1	36.2	58.8	269.1	326.8	2.6	44.1	2.9
9	Turonian	Channel and Tarling (1975)	*4.4*	*2.8*	*8.2*	*20.8*	5.5	20.8	59.2	249.3	334.8	5.9	34.2	8.5
10	Turonian–Coniacian	Channel et al. (1977)	*4.1*	*1.8*	*4.1*	*12.6*	4.4	10.9	59.4	247.2	335.8	4.3	33.5	6.3
11	Neocomian–Aptian	Van den Berg et al. (1993)	*3.2*	*2.6*	*7.3*	*43.9*	3.2	42.3	48.8	274.0	316.2	3.5	39.2	4.5
12	Priabonian	Márton et al. (2011)	*6.7*	*2.8*	*8.4*	*13.3*	4.6	27.6	85.7	106.9	5.7	8.8	59.7	5.9
13	Lutetian	Márton et al. (2011)	*6.3*	*4.1*	*14.9*	*37.5*	6.2	39.0	67.1	253.6	338.9	7.0	44.2	8.0
14	Ypresian	Márton et al. (2011)	*4.3*	*2.5*	*7.1*	*23.4*	4.0	26.9	62.1	251.1	336.0	4.6	38.3	6.1
15	Paleocene	Márton et al. (2011)	***3.3***	***3.9***	*13.8*	*116.8*	3.8	90.9	63.0	216.4	351.1	3.4	27.8	5.5
16	Maastrichtian	Márton et al. (2010)	***2.9***	***4.3***	*16.3*	***210.2***	2.7	239.5	56.1	233.0	340.6	3.0	22.0	5.2
17	Campanian	Márton et al. (2010)	***2.1***	***3.1***	*9.8*	***168.0***	2.1	164.2	62.5	241.9	339.9	2.2	35.0	3.2
18	Upper Coniacian	Márton et al. (2010)	***2.6***	***2.7***	*8.0*	*76.2*	2.8	67.8	62.9	243.2	339.6	2.8	35.9	3.9
19	Coniacian	Márton et al. (2010)	*3.4*	*2.9*	*8.9*	*52.3*	3.2	59.3	56.3	244.0	335.3	3.5	27.8	5.7
20	Turonian–Coniacian	Márton et al. (2010)	***2.0***	***2.6***	*7.6*	*113.7*	2.0	121.7	55.3	248.7	332.5	2.1	29.1	3.3
21	Cenomanian	Márton et al. (2010)	*3.1*	*2.6*	*7.3*	*47.5*	2.8	57.4	55.3	246.1	333.6	3.2	27.5	5.2
22	Valanginian–Hauterivian	Márton et al. (2010)	*4.8*	*2.8*	*8.2*	*23.4*	4.3	28.8	42.2	274.7	310.3	5.1	33.7	7.4
23	Berriasian	Márton et al. (2010)	***3.2***	***3.9***	*13.8*	*124.5*	3.3	116.3	39.1	276.3	307.0	3.4	32.1	5.0
24	Lutetian	Márton et al. (2003)	*7.1*	*2.9*	*8.7*	*12.8*	6.3	15.6	69.0	258.4	339.0	8.1	47.4	8.4
25	Cuisian	Márton et al. (2003)	*8.1*	*3.1*	*9.8*	*11.8*	7.1	15.2	69.2	240.4	344.5	8.9	42.3	10.7
26	Turonian–Coniacian	Márton et al. (2008)	*5.7*	*2.7*	*7.8*	*16.1*	4.4	25.9	67.4	269.2	334.9	6.6	50.1	6.4
27	Turonian	Márton et al. (2008)	*3.6*	*3.0*	*9.1*	*50.0*	3.1	65.2	68.1	245.2	342.3	4.0	42.4	4.7
28	Cenomanian	Márton et al. (2008)	***7.7***	*2.5*	***7.1***	*8.0*	5.7	13.6	79.6	271.3	347.4	9.7	56.6	7.4
29	Albian	Márton et al. (2008)	*3.2*	*2.3*	*6.0*	*32.2*	3.1	33.1	58.5	253.2	332.6	3.4	35.3	4.8
30	Valanginian–Aptian	Márton et al. (2008)	*6.0*	*3.1*	*9.8*	*20.7*	5.6	24.1	49.9	269.3	319.1	6.4	36.6	8.8
31	Tithonian	Márton et al. (2008)	*3.9*	*3.9*	*13.8*	*85.6*	3.9	85.3	50.8	274.3	317.9	4.3	41.0	5.3

SED
6, 937–983, 2014

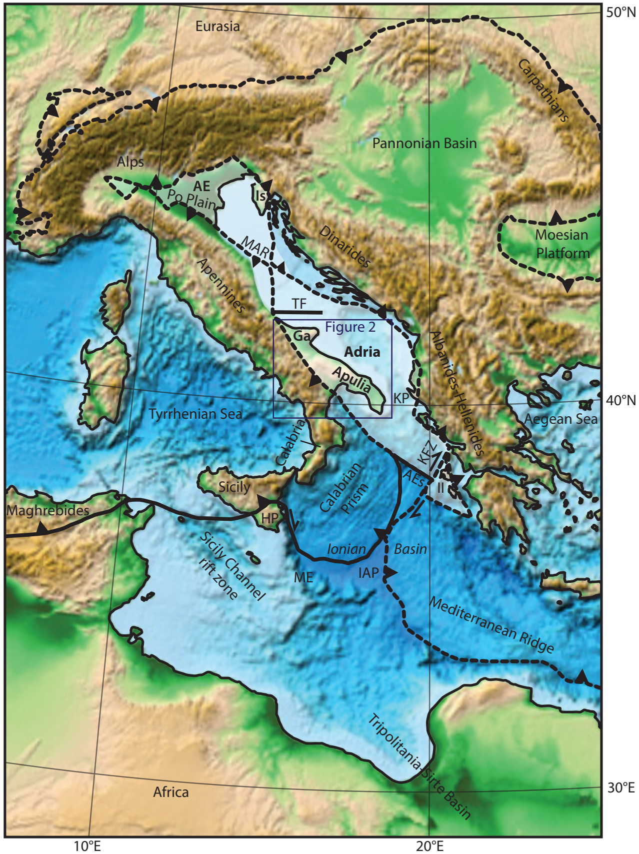

Fig. 1. Regional tectonic map of the Mediterranean region. AE = Adige Embayment; AEs = Apulian Escarpment; Ga = Gargano; HP = Hyblean Plateau; IAP = Ionian Abyssal Plain; II = Ionian Islands; Is = Istria; KFZ = Kefallonia Fault Zone; KP = Karaburun Peninsula; MAR = Mid-Adriatic Ridge; ME = Malta Escarpment; TF = Tremiti Fault.

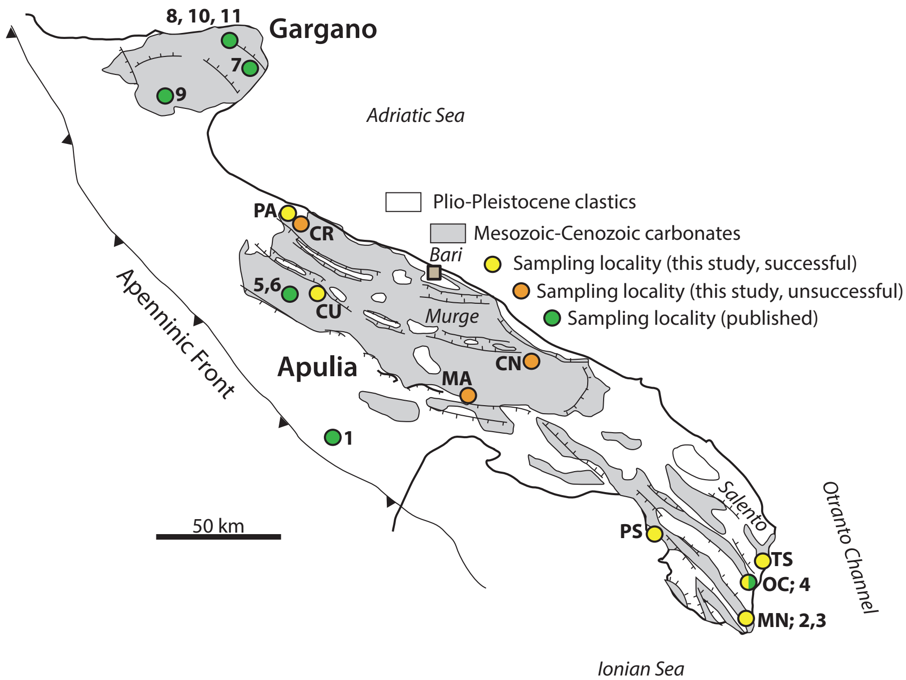

Fig. 2. A simplified geological map of the exposed Apulian Foreland (Apulia, southern Italy) indicating our new, and previously published paleomagnetic sampling sites (modified from Pieri et al., 1997). Numbers and codes correspond to sites listed in Table 1.

SED
6, 937–983, 2014

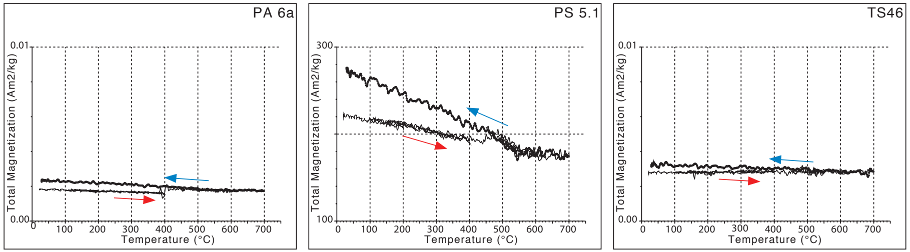

Fig. 3. Thermomagnetic curves measured on a Curie balance (Mullender et al., 1993) for representative samples. Arrows indicate heating (red) and cooling (blue).

SED
6, 937–983, 2014

Did Adria rotate relative to Africa?

D. J. J. van Hinsbergen et al.

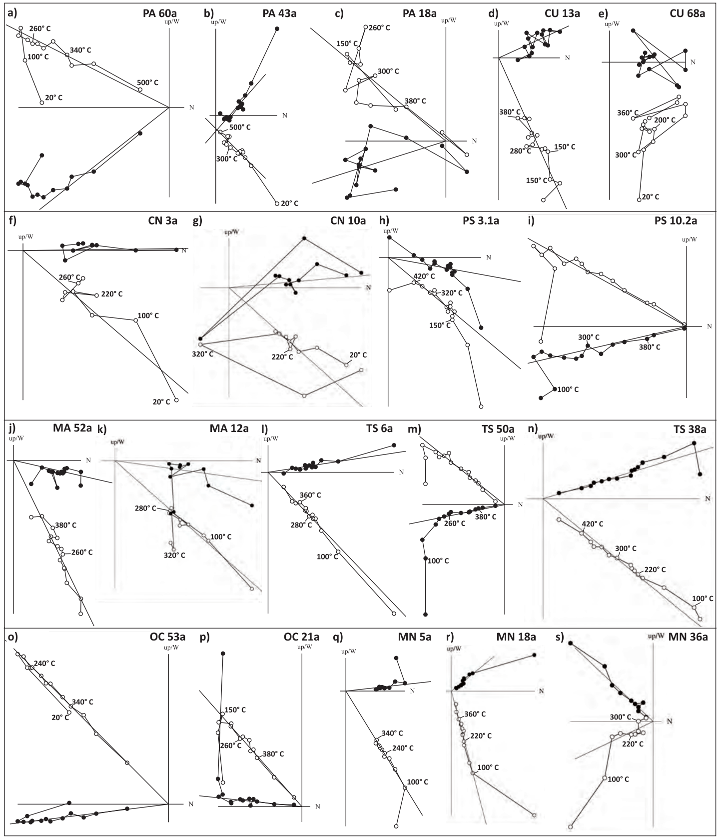

Fig. 4. Orthogonal vector diagrams (Zijderveld, 1967), showing representative demagnetization diagrams for all sampled sites. Except for OC, TS and MN all sites are in tilt corrected coordinates. Closed (open) circles indicate the projection on the horizontal (vertical) plane.

SED
6, 937–983, 2014

Did Adria rotate relative to Africa?

D. J. J. van Hinsbergen et al.

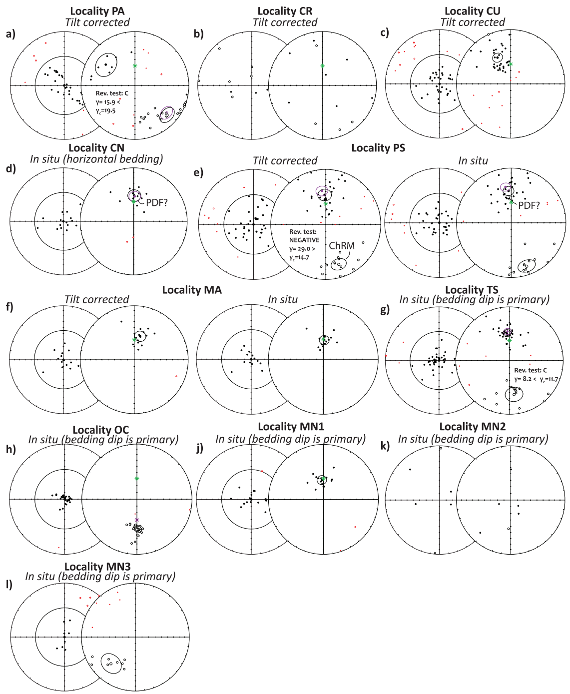

Fig. 5. Equal area projections of the VGP (left) and ChRM directions (right) of all sites in both in situ and tilt corrected coordinates. Open (closed) symbols corresponds to the projection on the upper (lower) hemisphere. Large dots in the ChRM plots indicate the mean direction and relative cone of confidence (α95). Red (small) dots indicate the individual directions rejected after applying a 45° cut-off. Green asterisk ($*$) indicates the present-day geocentric axial dipole (GAD) field direction at the sampled location. Sites TS, OC, and MN were sampled in sediments with a primary bedding attitudes, and should be considered in in situ coordinates.

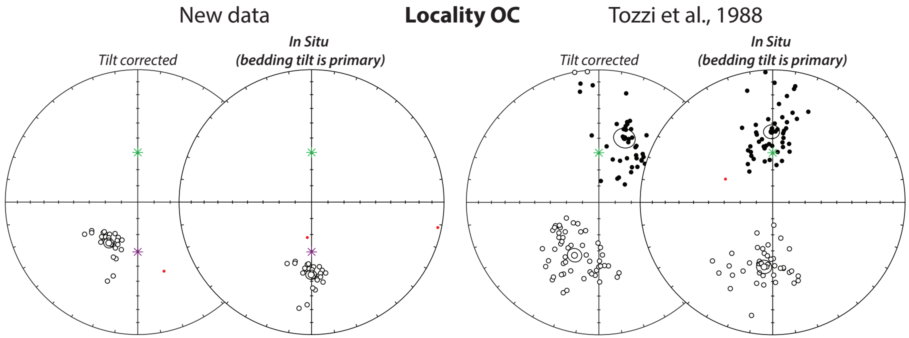

Fig. 6. Equal area projections of both in situ and tilt corrected ChRMs from our site OC (left) and from the same locality of Tozzi et al. (1988) (right), illustrating the apparent clockwise rotation that would result from a tilt correction of the bedding at this locality. The strata here have a primary dip (Fig. 7) and should be considered in in situ coordinates. Symbols are as in Fig. 5.

SED
6, 937–983, 2014

Did Adria rotate relative to Africa?

D. J. J. van Hinsbergen et al.

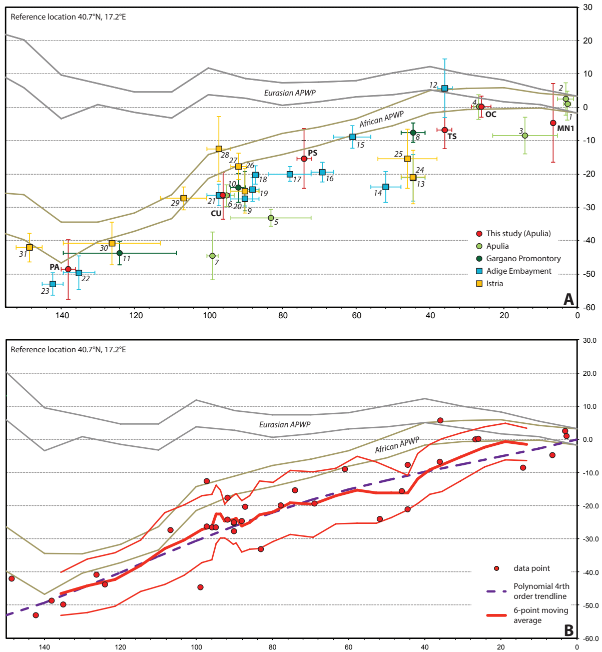

Fig. 7. (A) Age (Ma, following the timescale of Gradstein et al., 2012) vs. declination plot for our new, and published data from Adria. The error envelope for the African and Eurasian APWPs are from Torsvik et al. (2012). Vertical error bars correspond to the ΔD calculated at each site (Table 1); horizontal error bars correspond to age uncertainty. All data are recalculated to a reference location (40.7° N, 17.2° E). Numbers and site abbreviations correspond to data entries in Table 1. **(B)** Same data, with a polynomial 4th order trend line (purple dashed line) and the declination component of a full-vector 6-point moving average with error bars (ΔD) (red line).

SED
6, 937–983, 2014

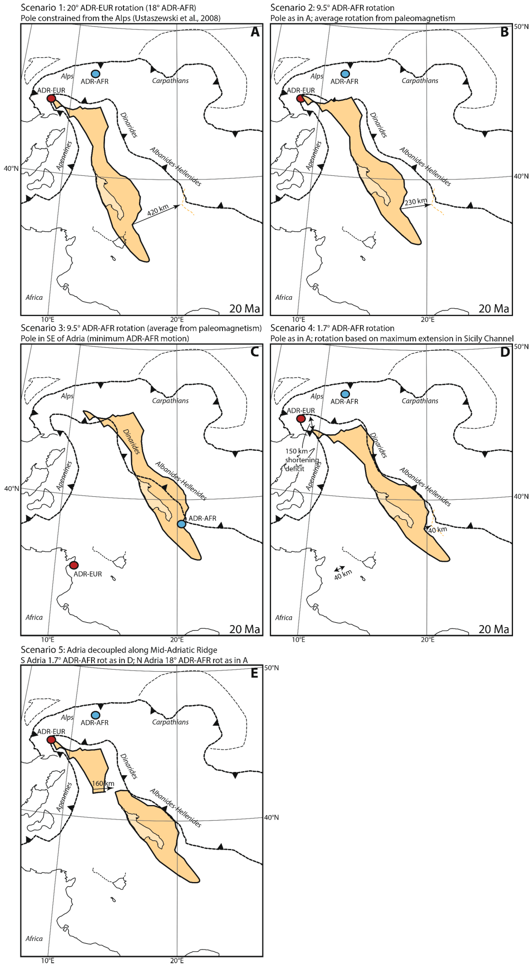

Fig. 8. Caption on next page.

SED
6, 937–983, 2014

Did Adria rotate relative to Africa?

D. J. J. van Hinsbergen et al.

Title Page
Abstract
Introduction
Conclusions
References
Tables
Figures
◀
▶
Back
Close
Full Screen / Esc
Printer-friendly Version
Interactive Discussion

Fig. 8. Reconstructions at 20 Ma for rotation scenarios of Adria vs. Africa that are permitted by paleomagnetic data, using **(A)** the rotation pole of Adria vs. Eurasia of Ustaszewski et al. (2008), and a 20° ccw rotation of Adria vs. Europe, corresponding to 18° ccw rotation of Adria vs. Africa, constrained from shortening reconstructions in the Alps by the same authors; **(B)** a 9.5° ccw rotation of Adria vs. Africa around the same pole corresponding to the paleomagnetically constrained mean rotation in this paper; **(C)** a 9.5° ccw rotation of Adria vs. Africa corresponding to the paleomagnetically constrained mean rotation in this paper, around a pole located in the SE of Adria and allowing minimum relative latitudinal motion between Africa and Adria; **(D)** a 1.7° ccw rotation of Adria vs. Africa around the pole of Ustaszewski et al. (2008), corresponding to the maximum amount of Neogene extension documented in the Sicily Channel; **(E)** decoupling north and south Adria along the Mid-Adriatic Ridge of Scisciani and Calamita (2009), with North Adria following a scenario as in **(A)**, and South Adria following a scenario as in **(D)**. Reconstructions of: (i) the Adriatic front of the Alps, Carpathians and Dinarides follow Ustaszewski et al. (2008), (ii) the western Mediterranean region follow Faccenna et al. (2004), and van Hinsbergen et al. (2014), and (iii) the Aegean–Albanian region follow van Hinsbergen and Schmid (2012). Reconstruction is given in a Europe-fixed frame, with the position of Africa determined using rotation poles of Gaina et al. (2002) and Müller et al. (1999) for the North Atlantic and Central Atlantic Ocean, respectively.

SED
6, 937–983, 2014